PROTECT 2024

# 9th International Colloquium on Performance, Protection & Strengthening of Structures Under Extreme Loading & Events

13th to 16th August 2024 at One Farrer Hotel in Singapore

# Advanced Engineered Composites in Protective Structures


**Vasant Matsagar, PhD**

**Professor, Dogra Chair, and Head**

Department of Civil Engineering

Indian Institute of Technology (IIT) Delhi


Monday, 4th March, 2024

# Agenda

## Basalt Fiber Products


Chopped fiber


Bar


Grid


Profile


Steel-fiber hybrid bar


Sheet


Roving


Laminate

# Basalt Fiber Reinforced Polymer (BFRP)

## Basalt fiber composite: A new engineered composite

- ➢ Structural sustainability and safety (more attention). Includes: durability of structures, recoverability after disasters, **use of new materials**, and economical issues.
- ➢ Financial loss due to corrosion of steel (sea water): up to **700 Billion USD** every year (Wu et al., 2012).

- ✓ Basalt fiber: made from basalt rock melted at 1400°C **without any additives.**
- ✓ One of the best alternatives to steel.

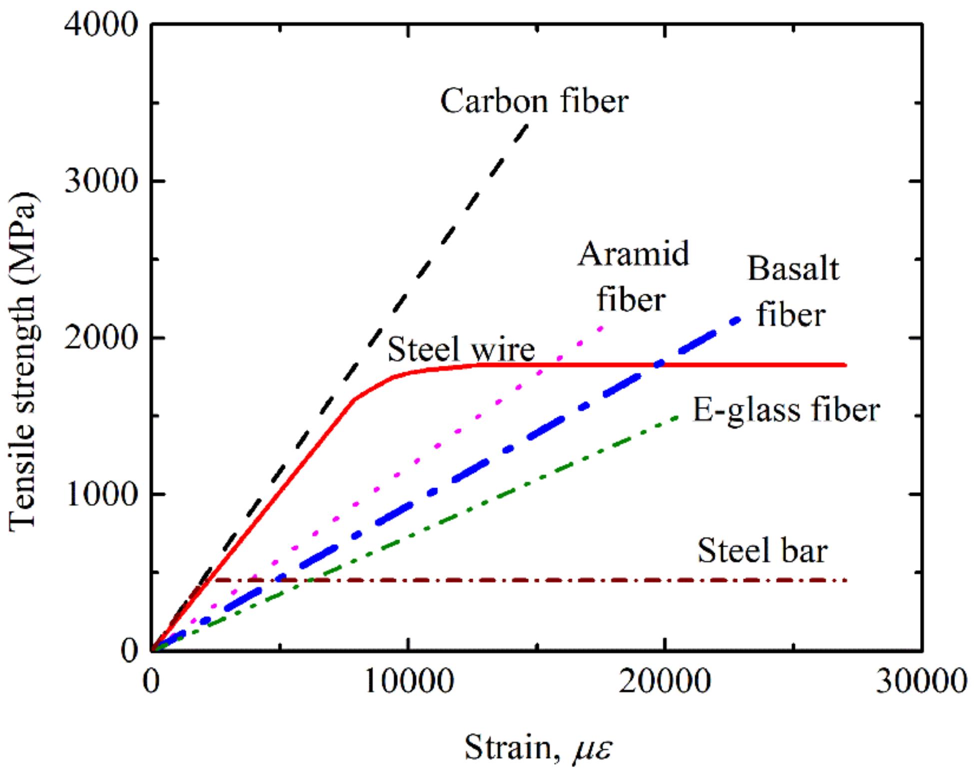


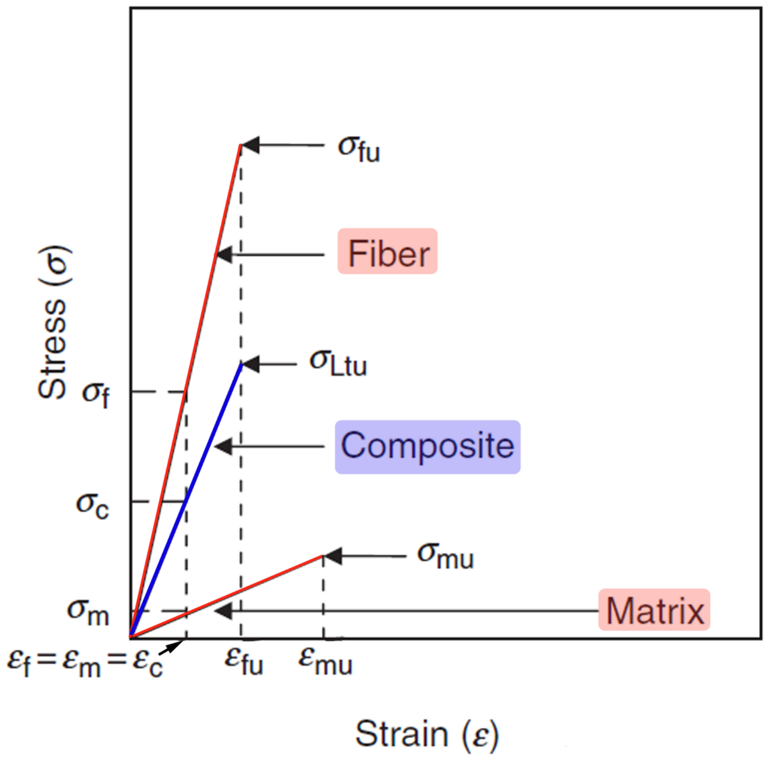

## Applications of FRP Composites


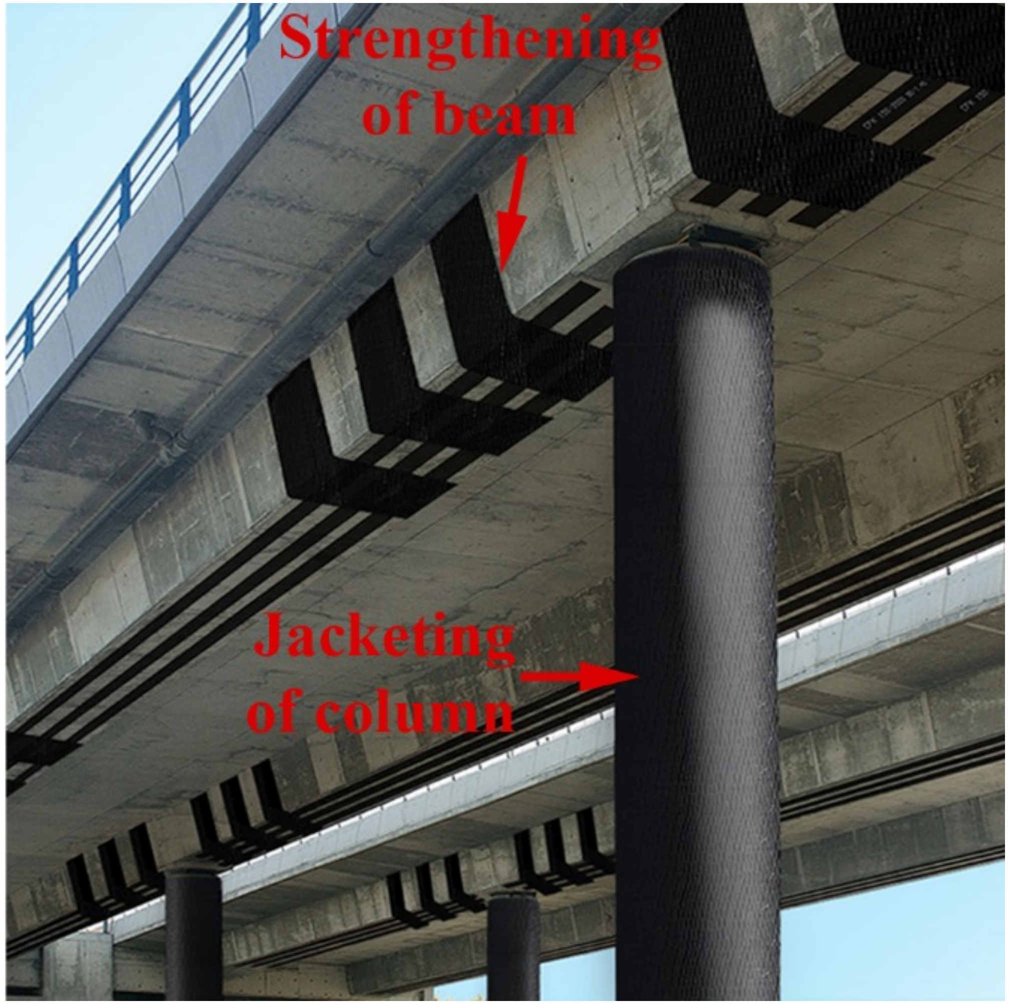

## General Applications

- Basalt Fiber Reinforced Polymer (BFRP) laminates can be installed in all types of structural applications including but not limited to flexural strengthening, shear strengthening, and axial confinement applications.
- Flexibility in usage is one of the most appealing aspects of the rehabilitation system

FRP used in flexural strengthening


FRP used in shear strengthening

FRP used in an axial confinement

## Characterization at Elevated Temperatures

**Motivation**

- Integral bridges experience thermal stresses throughout their service life.
- The thermo-mechanical behavior of the BFRP composites varies with the manufacturing.

**Tensile strength**

- No degradation at 250°C (Wu et al., 2011)
- No obvious change close to $T_g$ (Zhu et al., 2014)
- Degradable after 100°C (Zhang et al., 2016)
- 30% degradation at 250°C (Hamad et al., 2017)

**Elastic modulus**

- 58% degradation at 250°C (Wu et al., 2011)
- No obvious change close to $T_g$ (Zhu et al., 2014)
- 12% degradation at 250°C (Hamad et al., 2017)

The absence of full investigations and understanding of the behavior of BFRP rebars at elevated temperatures raises the need for further research study to compliment the state-of-the-art and contribute to international standards on this subject.

# Basalt Fiber Reinforced Polymer (BFRP)

## Characterization at Elevated Temperatures: Prerequisite Tests

### Properties of the BFRP Rod

Fiber volume fraction ($v_f$), glass transition temperature ($T_g$) and resin decomposition temperature ($T_d$) are not mentioned in the data sheet.

| Property | Parameter |
|---|---|
| Nominal diameter of rod (mm) | 8 |
| Tensile strength (MPa) | 1125 |
| Tensile modulus of elasticity (GPa) | 52 |
| Transverse modulus of elasticity (GPa) | 3.48 |
| Shear modulus (GPa) | 1.24 |
| Strain at break | 0.0235 |

**Missing properties are required for the thermo-mechanical study.**

### 1. Determination of fiber content

The SEM analysis is performed at a scale bar of 100-micron and 50-micron.

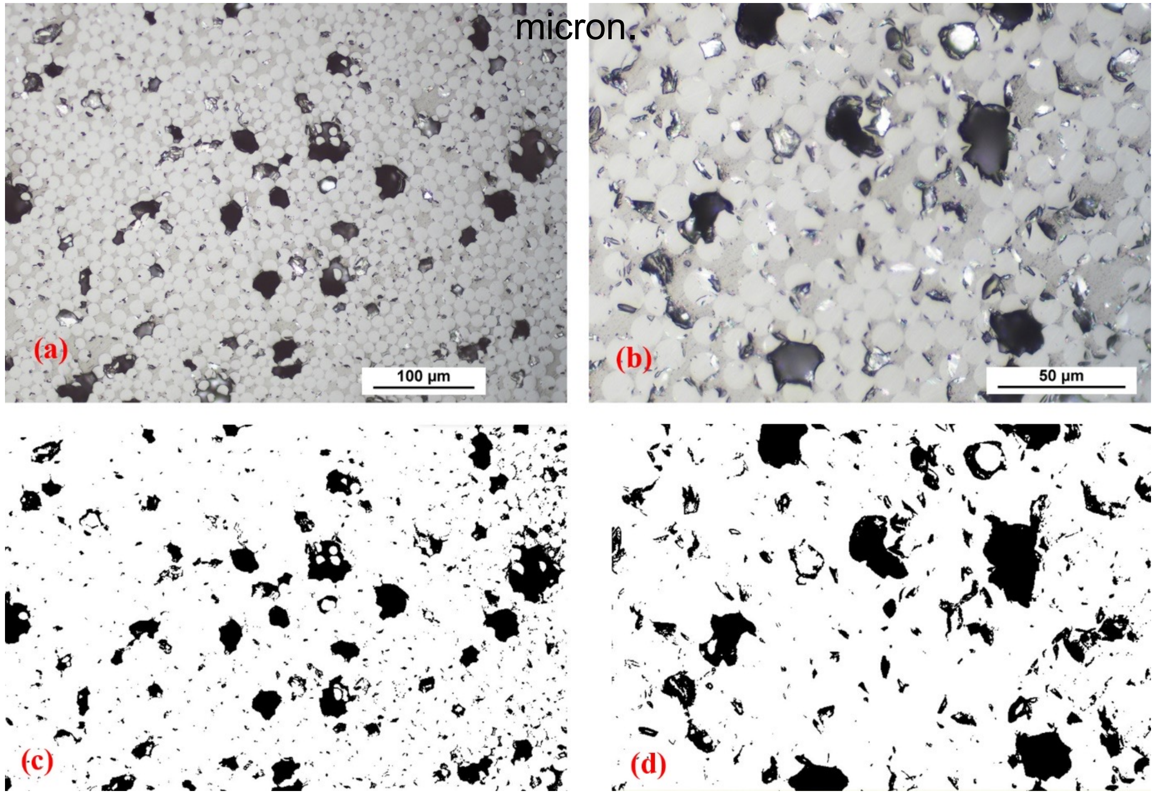


- The scanning electron microscopy (SEM) analysis is conducted on 12 BFRP rod specimens.
- The average fiber content is found to be 80.1%.

## Characterization at Elevated Temperatures: Prerequisite Tests

### 2. Glass transition temperature ($T_g$)

- Dynamic mechanical thermal analysis (DMTA) test.
- **$T_g$ of the resin is found to be 171.7°C.**

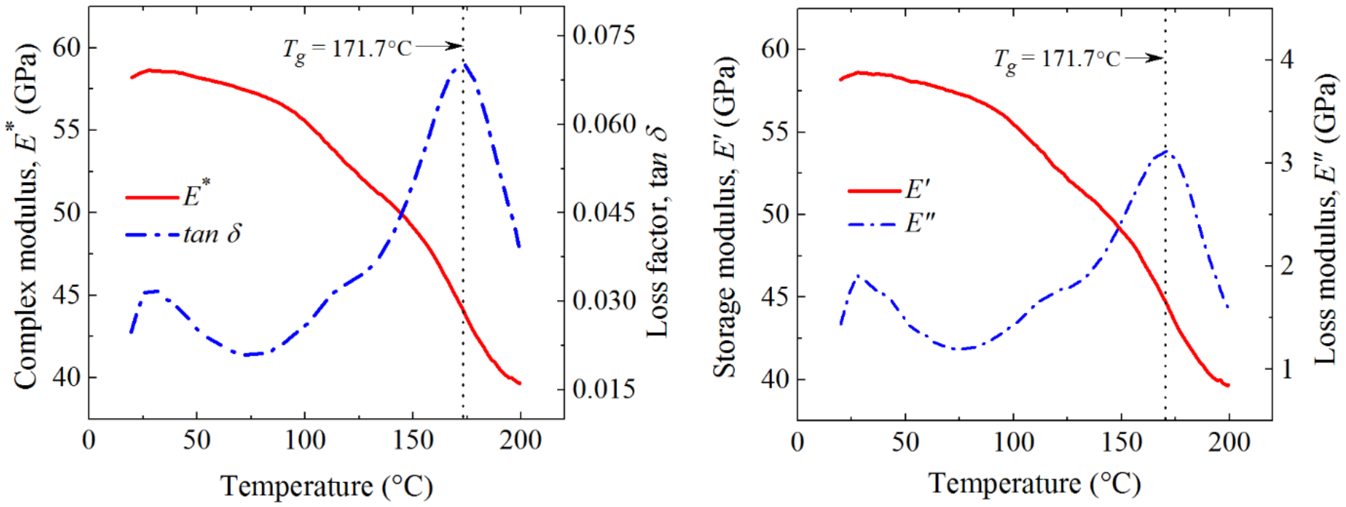


### 3. Resin decomposition temperature ($T_d$)

- Thermo-gravimetric analysis (TGA) test.
- **$T_d$ is found to be 423.7°C.**

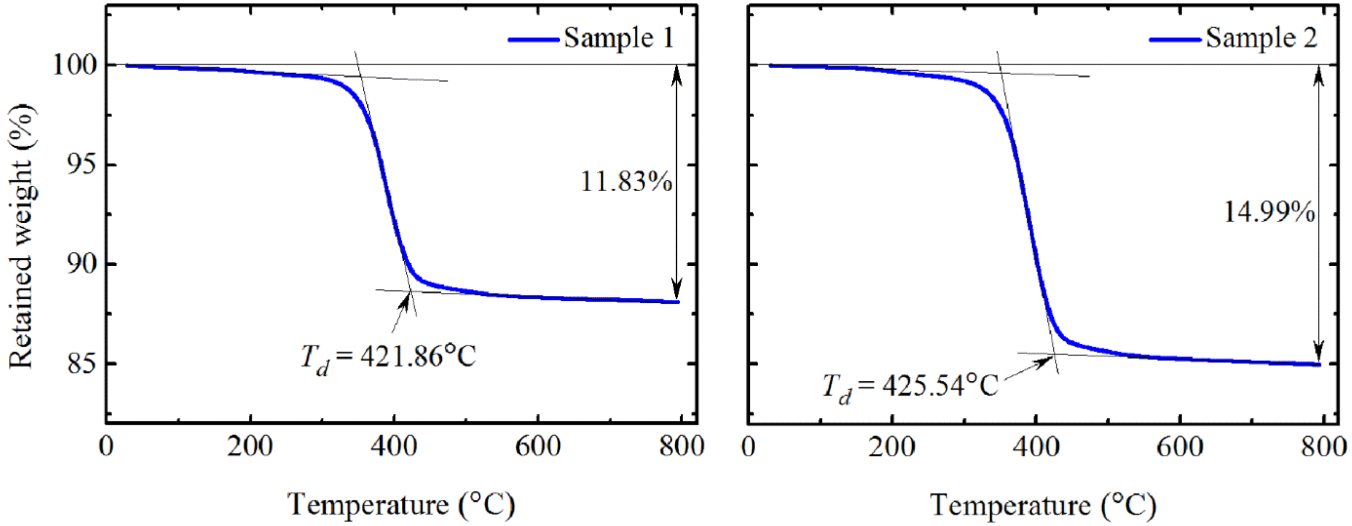

## Characterization at Elevated Temperatures: Prerequisite Tests

### 4. Measurement of Elastic Modulus

- Using extensometer in tension test at elevated temperatures is challenging.
- Total elongation of BFRP rod sample can also be used if proved reliable.
- Total elongation-based approach is found reliable with 6.9% error.

Tension test at ambient temperature

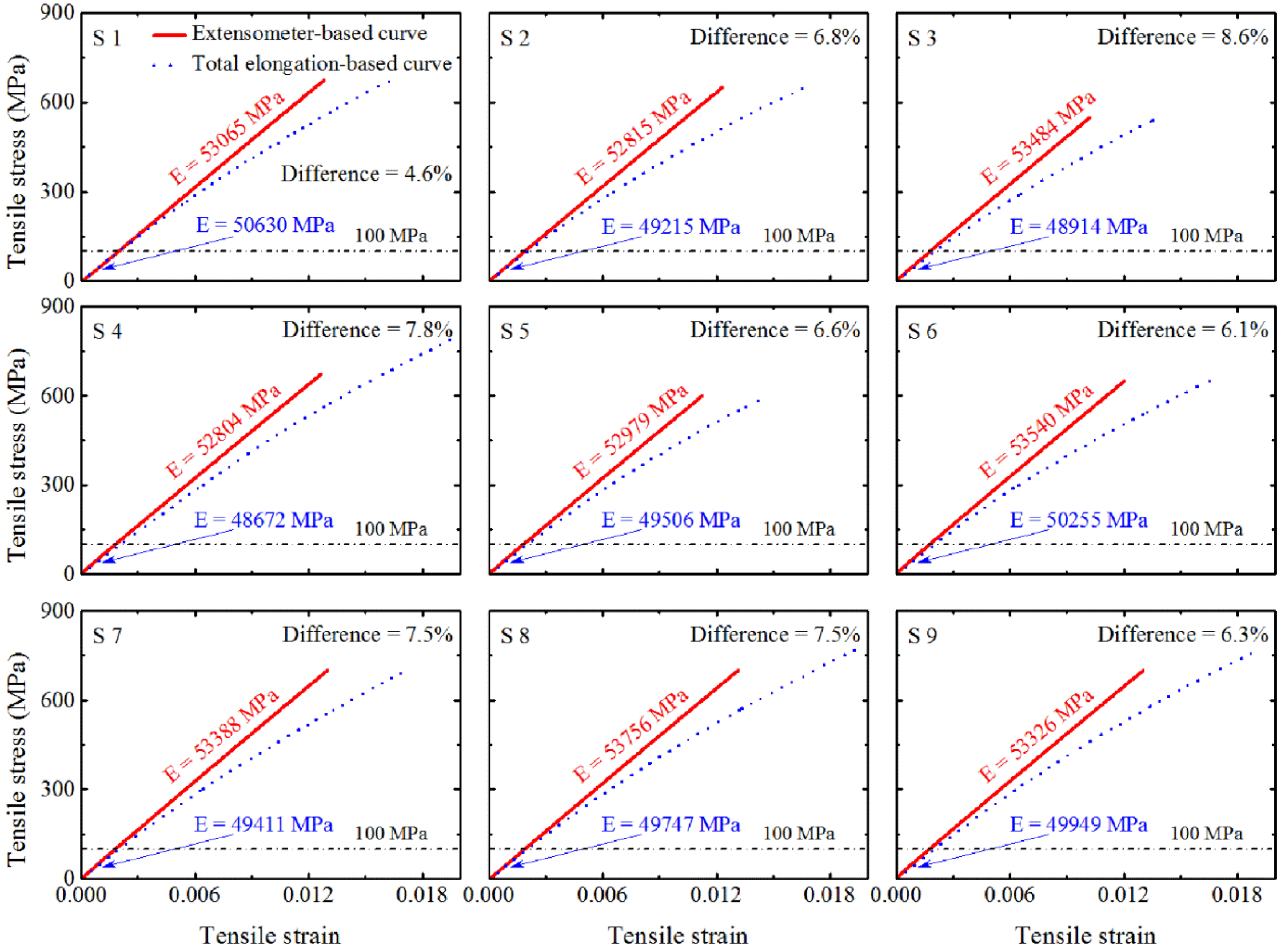

## Tension Test on BFRP at Elevated Temperatures

Total of 30 BFRP rod samples are tested, three identical specimens at each temperature level.


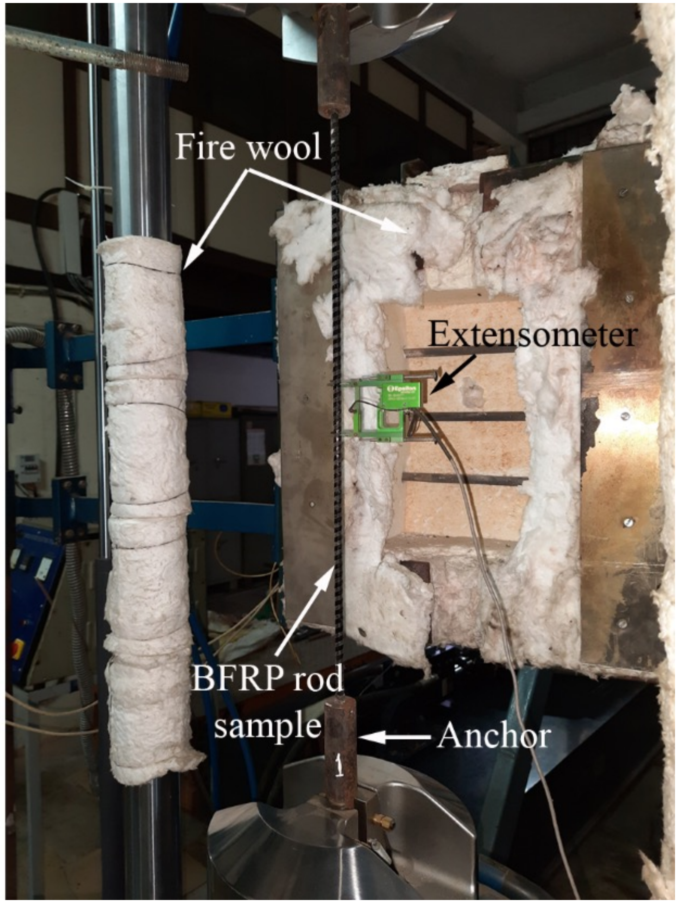



## Tension Test on BFRP rod at Elevated Temperatures

- Load-deflection response is considered for evaluating the degradation in tensile strength and stiffness with temperature.
- Mild degradation up to 200°C.
- More pronounced degradation after 200°C, up to 400°C.
- Total loss of tensile strength at 450°C.

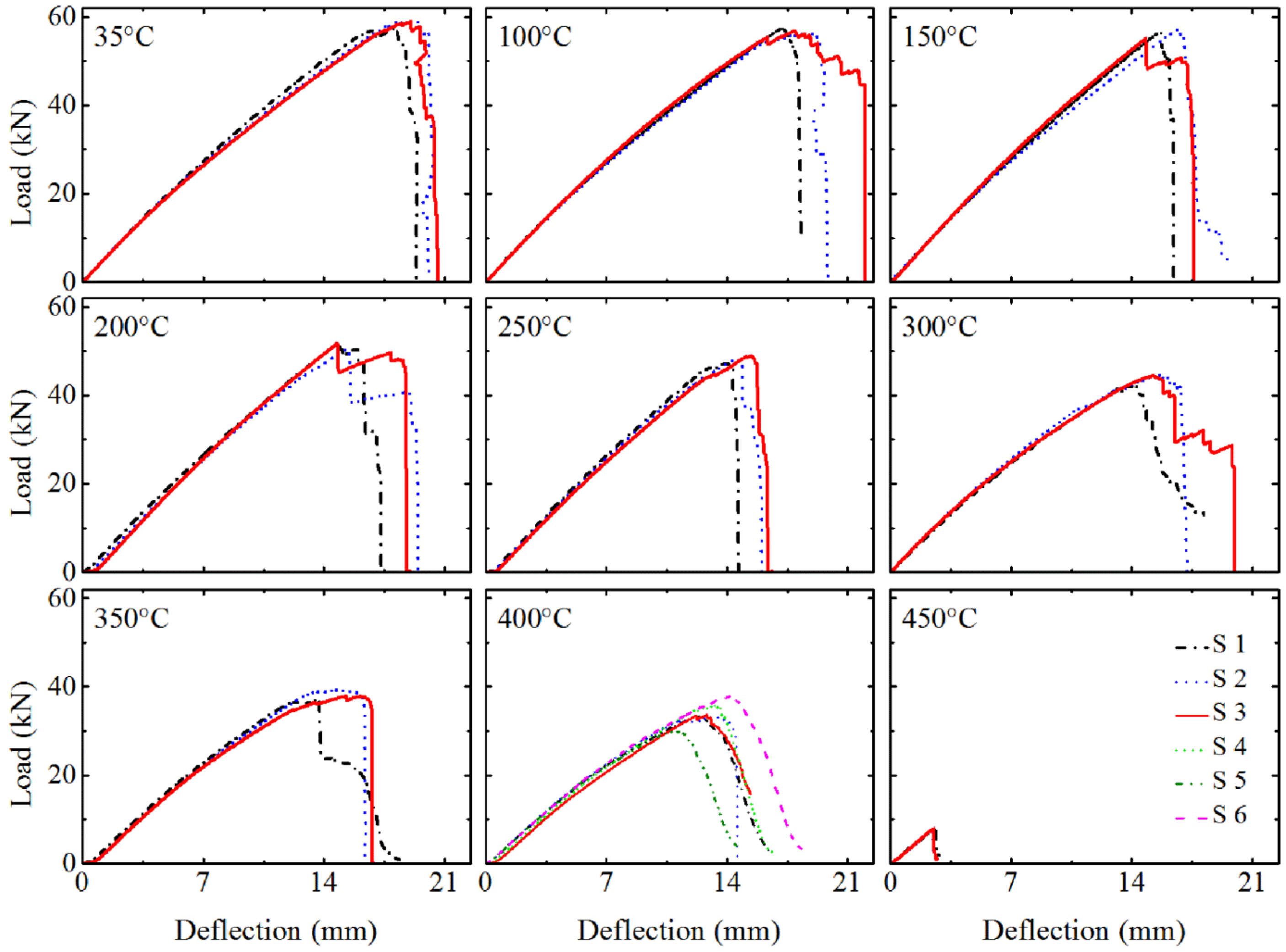

# Tension Test on BFRP rod at Elevated Temperatures

**Degradation in Tensile Strength and Tensile Modulus of Elasticity**

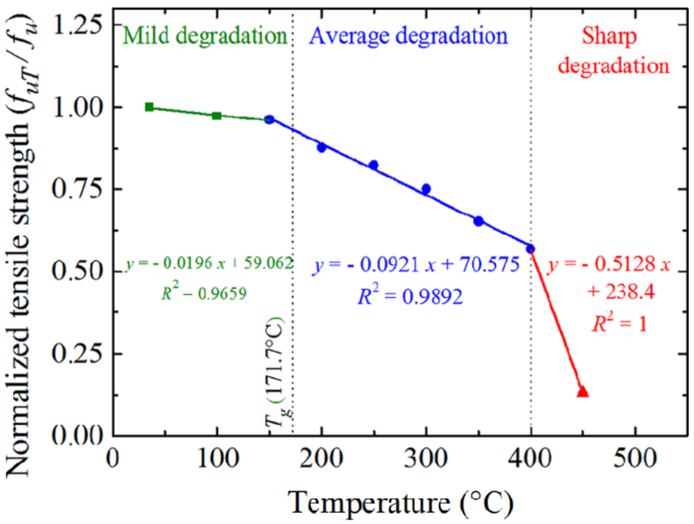


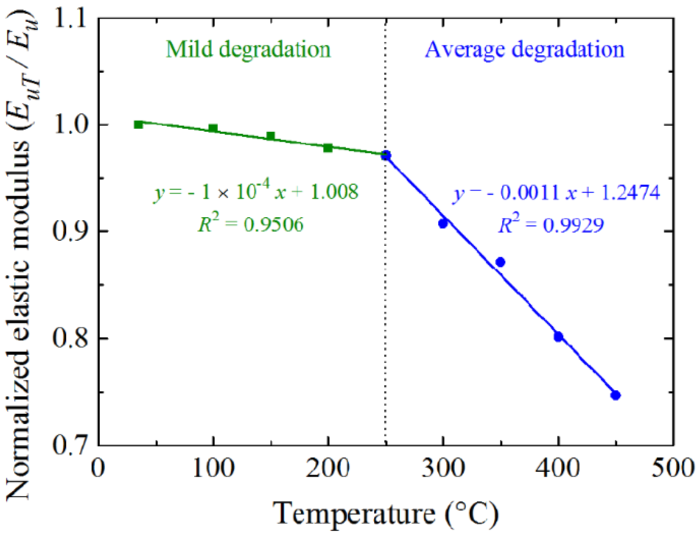


**Performance Assessment on BFRP Rod at Elevated Temperatures**

- ➢ The BFRP rod, tested in the current study, has performed remarkably.

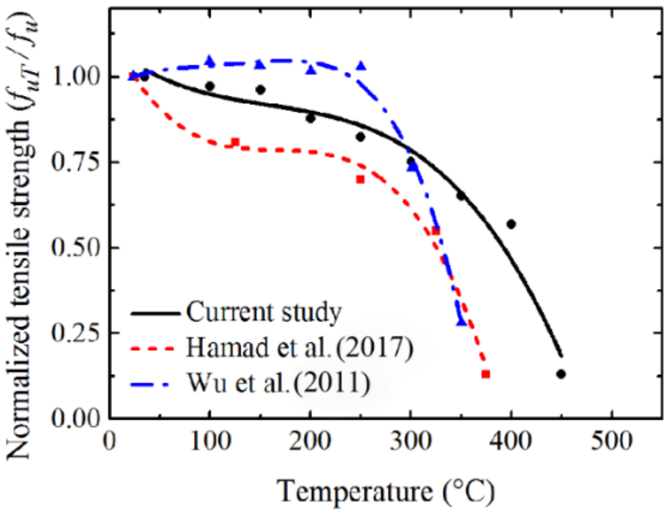


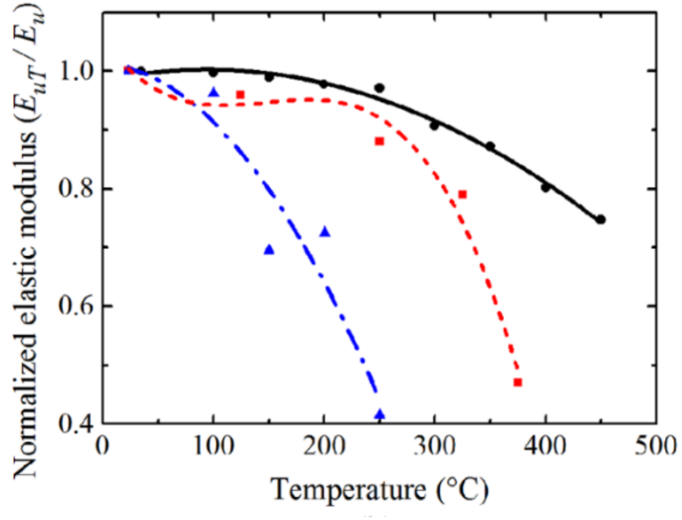

# Basalt Fiber Reinforced Polymer (BFRP)

## Scanning Electron Microscopy (SEM)

- The scanning electron microscopy (SEM) investigation is carried out on three rod samples tested at different temperature levels.

- The good bonding can be observed at room temperature (35°C) where a bundle of fibers can be seen.

- The discreteness of fibers can be seen at 250°C and 450°C.

- The smooth surfaces of fiber, free of resin, can be seen at 450°C.

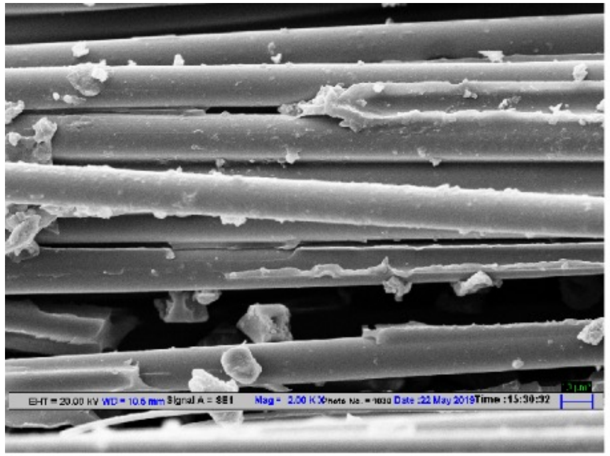

35°C

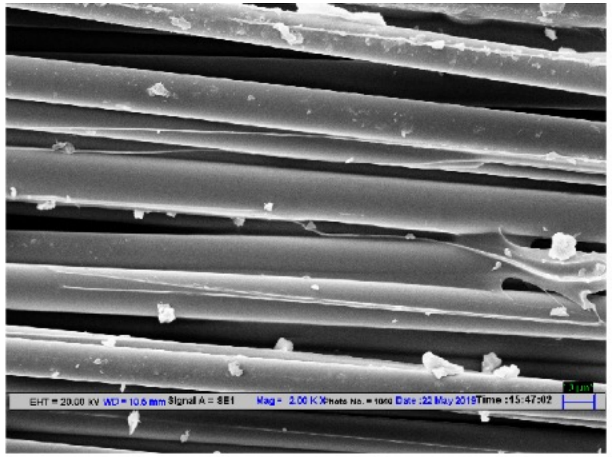

250°C

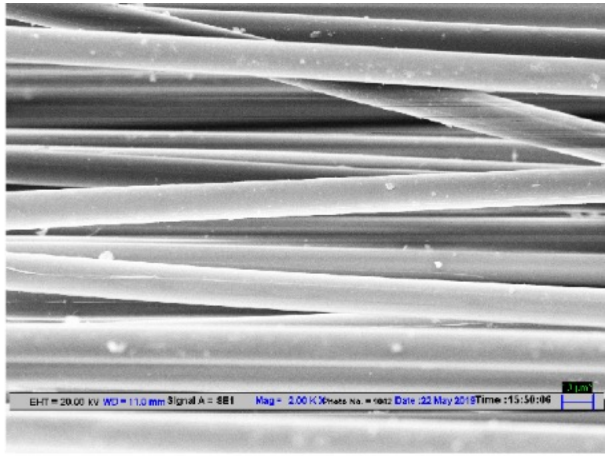

450°C

# Basalt Fiber Reinforced Polymer (BFRP)

## Development of Constitutive Law

Three existing approaches as well as an initial proposed model are fitted with the experimental results.

1. Gu and Asaro (2004)

$$P(T) = P_0\left(1 - \frac{T - T_0}{T_{ref\_}T_0}\right)^m$$

2. Liu et al. (2005)

$$\frac{P_T}{P_0} = 1 - a_1\left(\frac{T - T_0}{T_g - T_0}\right) - a_2\left(\frac{T - T_0}{T_g - T_0}\right)^2 - a_3\left(\frac{T - T_0}{T_g - T_0}\right)^3$$

3. Corriea et al. (2013)

$$P(T) = \left(1 - e^{Be^{CT}}\right) \times \left(P_0 - P_r\right) + P_r$$

4. Proposed model

$$P(T) = P_0\left(1.507 - 0.507\exp\left\{\left[\frac{T - T_0}{T_d}\right]^{2.142}\right\}\right)$$

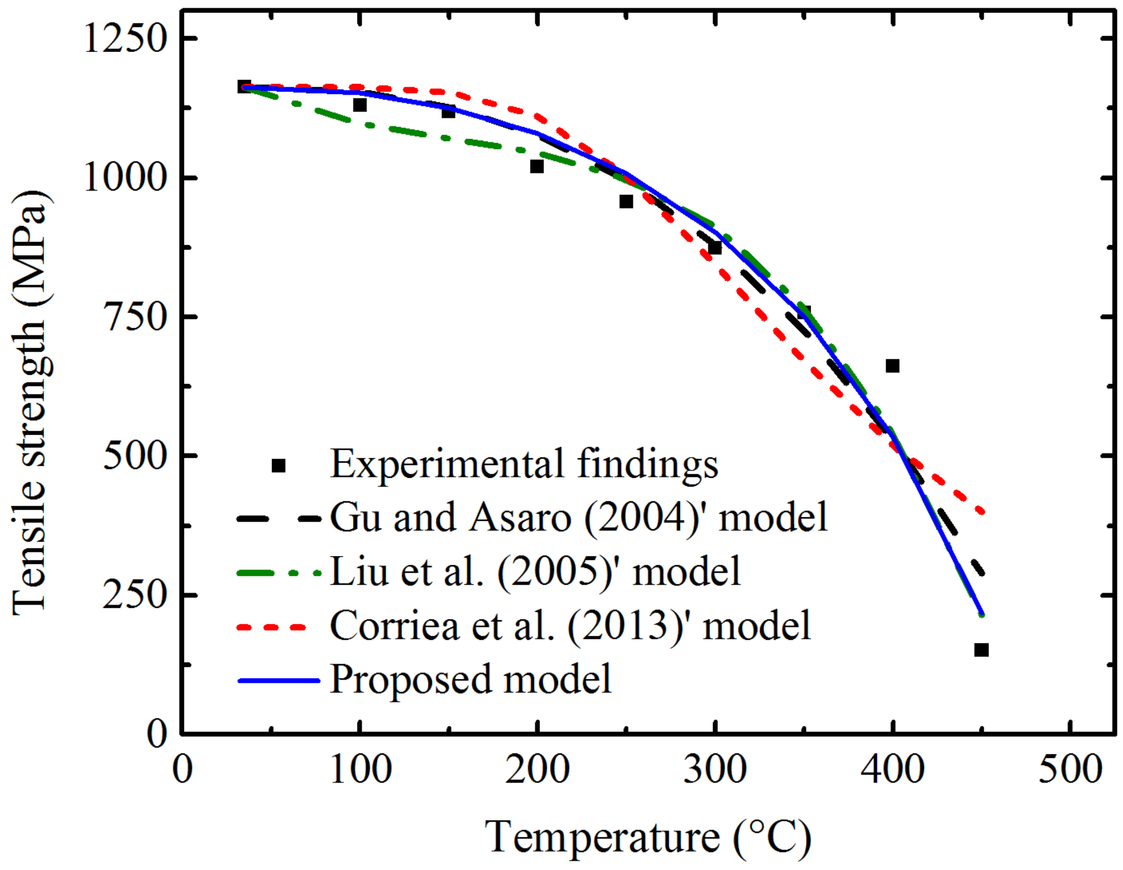

## Development of Constitutive Law

$$P(T) = P_0\left(A - (A-1)\exp\left\{\left[\frac{T - T_0}{T_d}\right]^C\right\}\right)$$

$$A = 0.0725\sqrt{T_d}$$

$$C = 0.154 v_f \exp(0.0166 T_g)$$

The proposed model:
original,
generic, and
flexible.

### Implementation

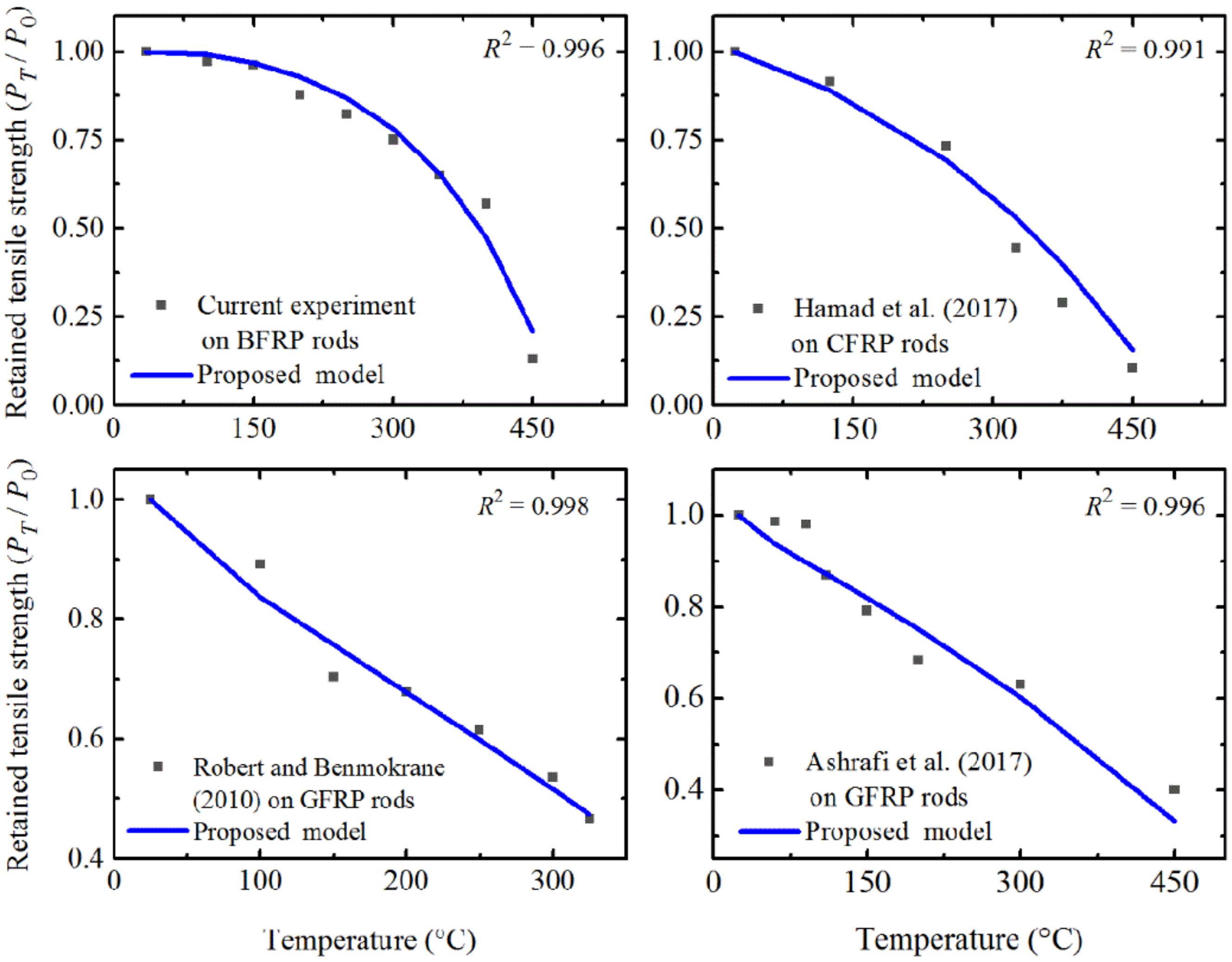

# Split Hopkinson Pressure Bar (SHPB)


Uniaxial Split Hopkinson Pressure Bar

- Bar Diameter = 76 mm,
- Bar Length = 3048 mm,
- Strain Rate Achieved = 100 – 1400 /s

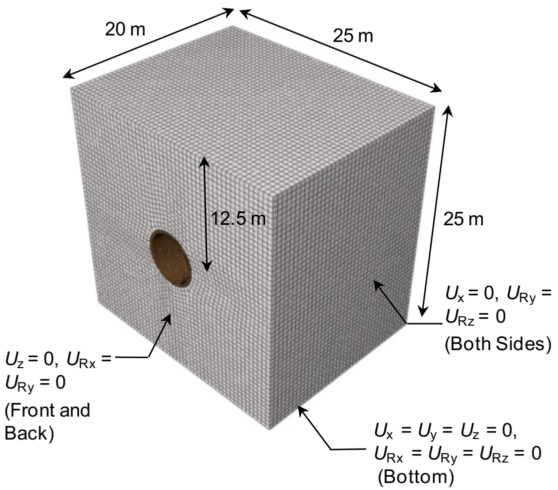


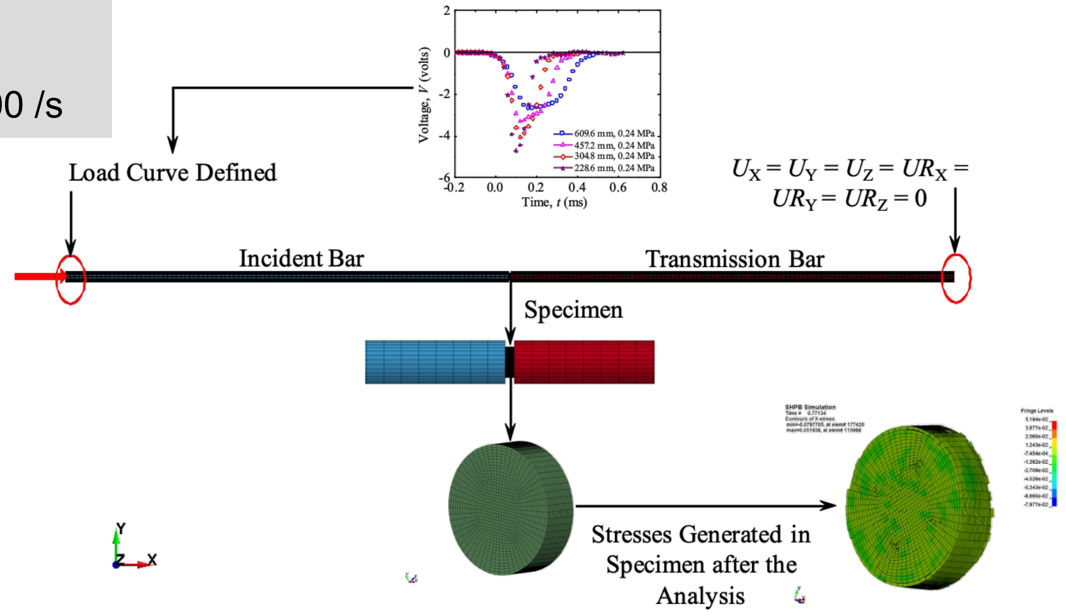


Design-development of **triaxial large diameter SHPB** system for structural materials

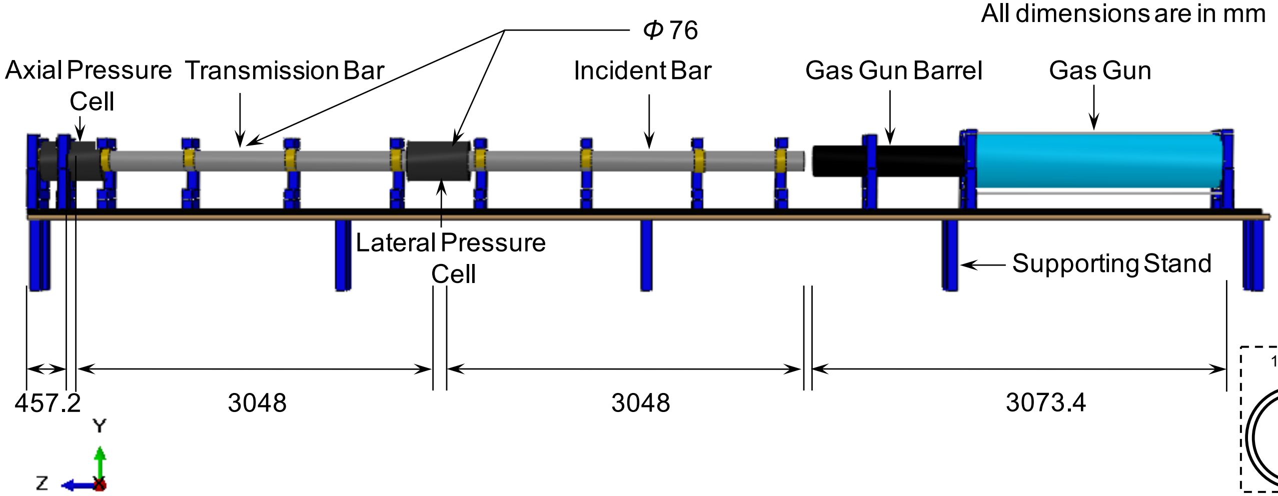


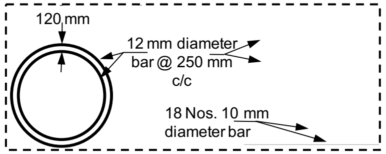


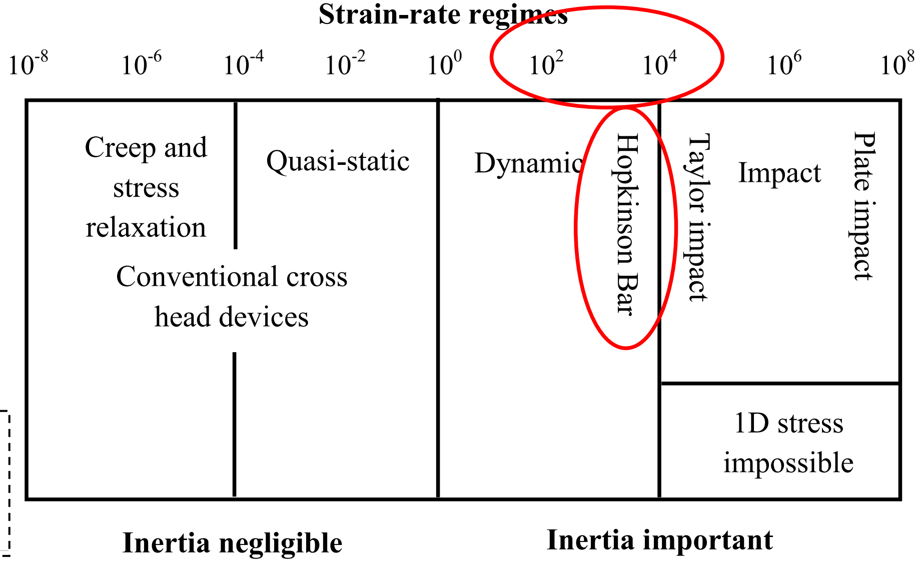

## Engineered composite: laminated composite plate

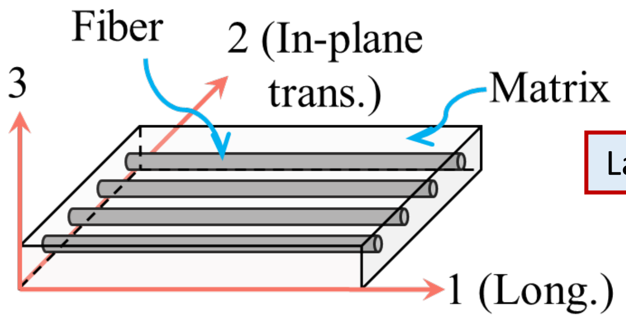


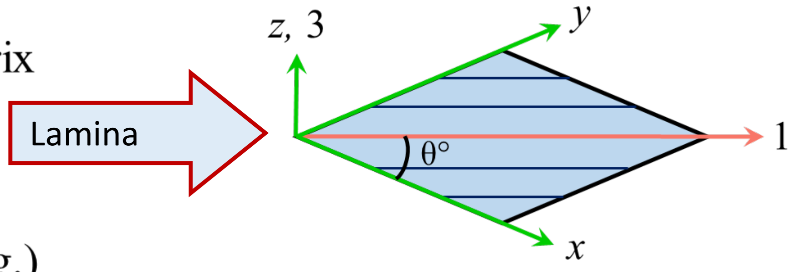


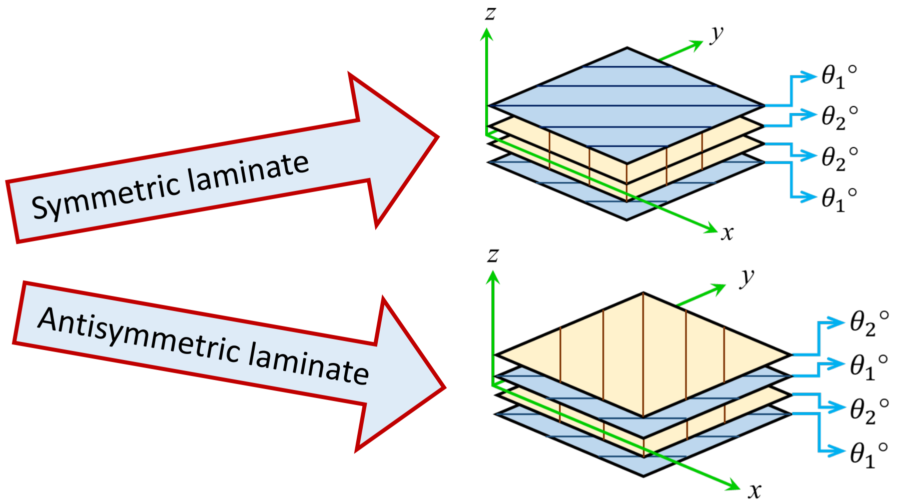


$$A_{ij} = \sum_{k=1}^{N} \left(\bar{Q}_{ij}\right)_k (z_k - z_{k-1})$$

$$B_{ij} = \frac{1}{2}\sum_{k=1}^{N} \left(\bar{Q}_{ij}\right)_k (z_k^2 - z_{k-1}^2)$$

$$D_{ij} = \frac{1}{3}\sum_{k=1}^{N} \left(\bar{Q}_{ij}\right)_k (z_k^3 - z_{k-1}^3)$$

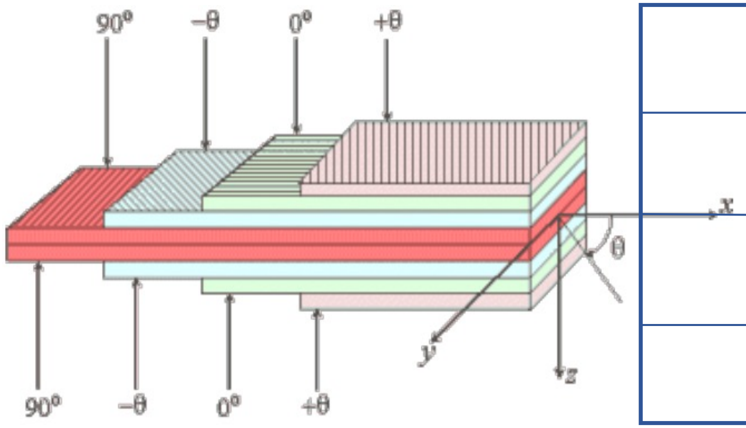


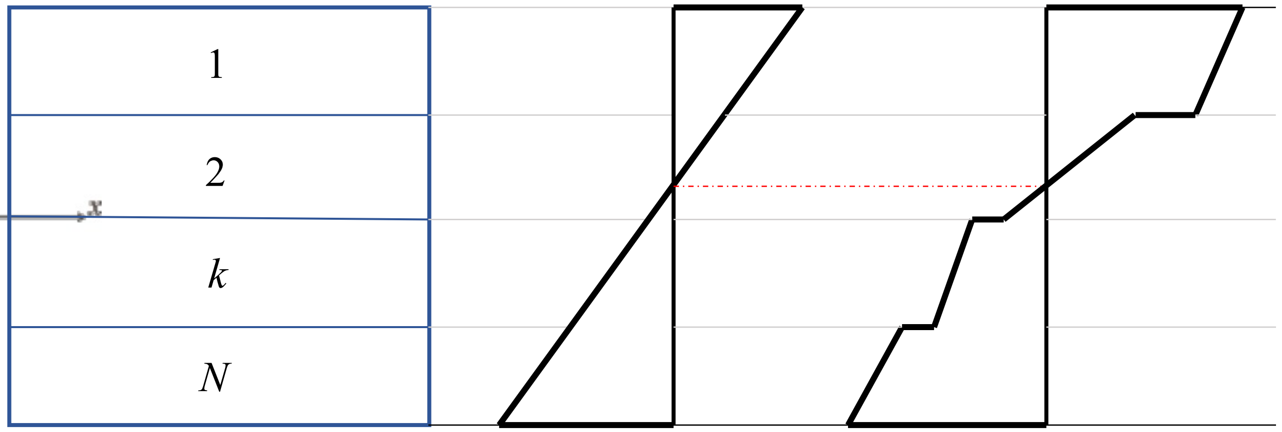


Laminate

Strain variation

Stress variation

Here, $N_i$ and $M_i$ are resultant forces and moments on the laminate, $\varepsilon_j$ and $\kappa_j$ are mid-plane strains and curvatures, $A_{ij}$ extensional stiffnesses, $B_{ij}$ coupling stiffnesses, and $D_{ij}$ bending stiffnesses.

## Finite element (FE) formulation of composite plate in thermal environments

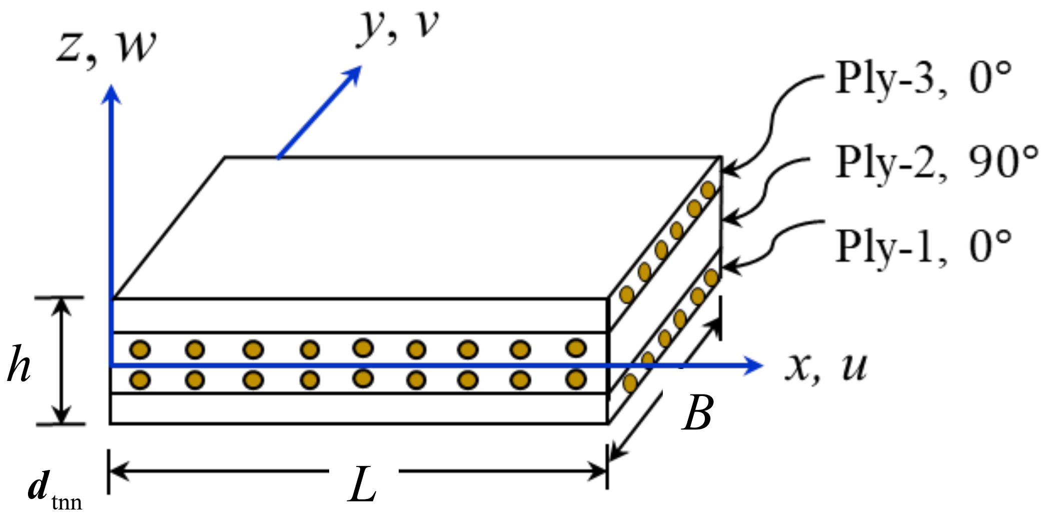


Constitutive Relation of laminate (using first order shear deformation theory):

$$\begin{Bmatrix} \sigma_x \\ \sigma_y \\ \tau_{xy} \end{Bmatrix}_k = \begin{bmatrix} Q_{11} & Q_{12} & Q_{16} \\ Q_{12} & Q_{22} & Q_{26} \\ Q_{16} & Q_{26} & Q_{66} \end{bmatrix}_k \begin{Bmatrix} \varepsilon_x \\ \varepsilon_y \\ \gamma_{xy} \end{Bmatrix}$$

and

$$\begin{Bmatrix} \tau_{yz} \\ \tau_{zx} \end{Bmatrix}_k = \begin{bmatrix} Q_{44} & Q_{45} \\ Q_{45} & Q_{55} \end{bmatrix}_k \begin{Bmatrix} \gamma_{yz} \\ \gamma_{zx} \end{Bmatrix}$$

### Hamilton's variational principle

$$\delta \int_{t_1}^{t_2} \mathcal{L}\mathrm{d}t = \int_{t_1}^{t_2} \delta(U - W - T)\mathrm{d}t = 0$$

wherein, variation of the total kinetic energy: $\delta T$

$$\delta T = \sum_{e=1}^{ne} \delta T_e = -\sum_{e=1}^{ne} \delta \mathrm{d}_e \left( \int_{A_e} \underbrace{(\boldsymbol{N}^{\mathrm{T}} \bar{\boldsymbol{M}} \boldsymbol{N} \mathrm{d}A_e)}_{\boldsymbol{M}} \right) \ddot{\boldsymbol{d}}_e$$

and, variation of the total potential energy: $\delta V = \delta(U - W)$

$$\delta V = \sum_{e=1}^{ne} \delta V_e = \sum_{e=1}^{ne} \left( \delta \int_{A_e} \underbrace{(\boldsymbol{d}_e^{\mathrm{T}} \boldsymbol{B}^{\mathrm{T}} \bar{\boldsymbol{D}} \boldsymbol{B} \boldsymbol{d}_e)}_{\boldsymbol{K}} \mathrm{d}A_e - \frac{1}{2} \delta \int_{A_e} \underbrace{(\boldsymbol{d}_e^{\mathrm{T}} \boldsymbol{G}^{\mathrm{T}} \boldsymbol{S}_r \boldsymbol{G} \boldsymbol{d}_e)}_{\boldsymbol{K_G}} \mathrm{d}A_e - \delta \int_{A_e} \underbrace{(\boldsymbol{d}_e^{\mathrm{T}} \boldsymbol{N}^{\mathrm{T}} q)}_{\boldsymbol{P}} \mathrm{d}A_e \right)$$

Thus, governing equation of composite plate in elevated temperature

$$(\boldsymbol{K} + \boldsymbol{K_G})\boldsymbol{d}_{\mathrm{tnn}} + \boldsymbol{M}\ddot{\boldsymbol{d}}_{\mathrm{tnn}} = \boldsymbol{P}$$

Here, $\boldsymbol{N}$: shape function, $t_{nn}$: total number of nodes in an element, $ne$: total number of elements, $\boldsymbol{d}_{\mathrm{tnn}}$: global displacement vector, and $\boldsymbol{q}$: external dynamic load vector

## Application of the FRP composite plate for strengthening concrete against blast load

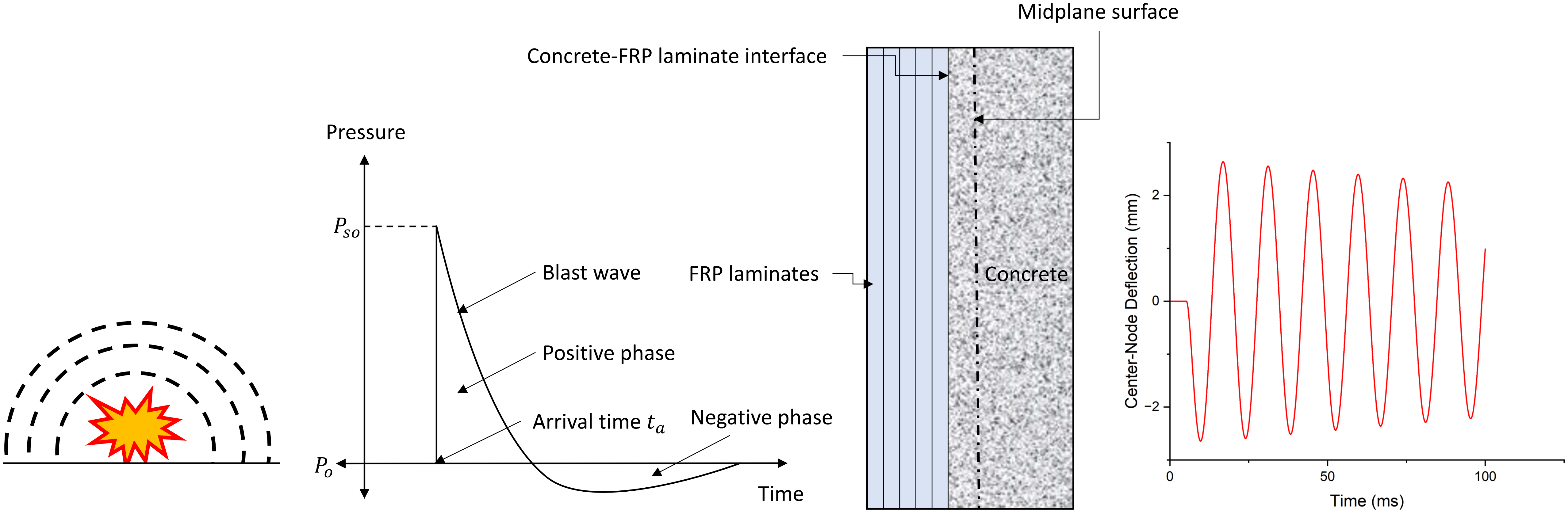


Computing blast wave parameters → Obtaining Blast Wave Profile → Computing ABD matrix using Classical Lamination Theory → Computing the dynamic response of the central node

# FRP Composite Plates under Blast load

## Validation with 3D-FE analysis for different radial distance from explosion center

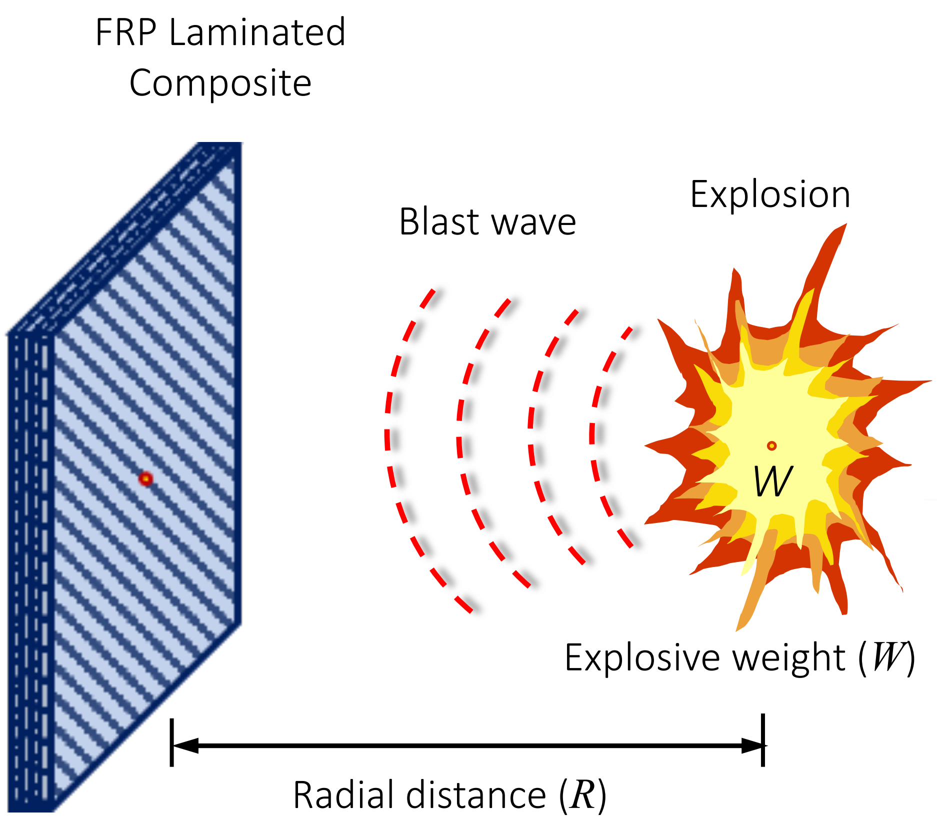


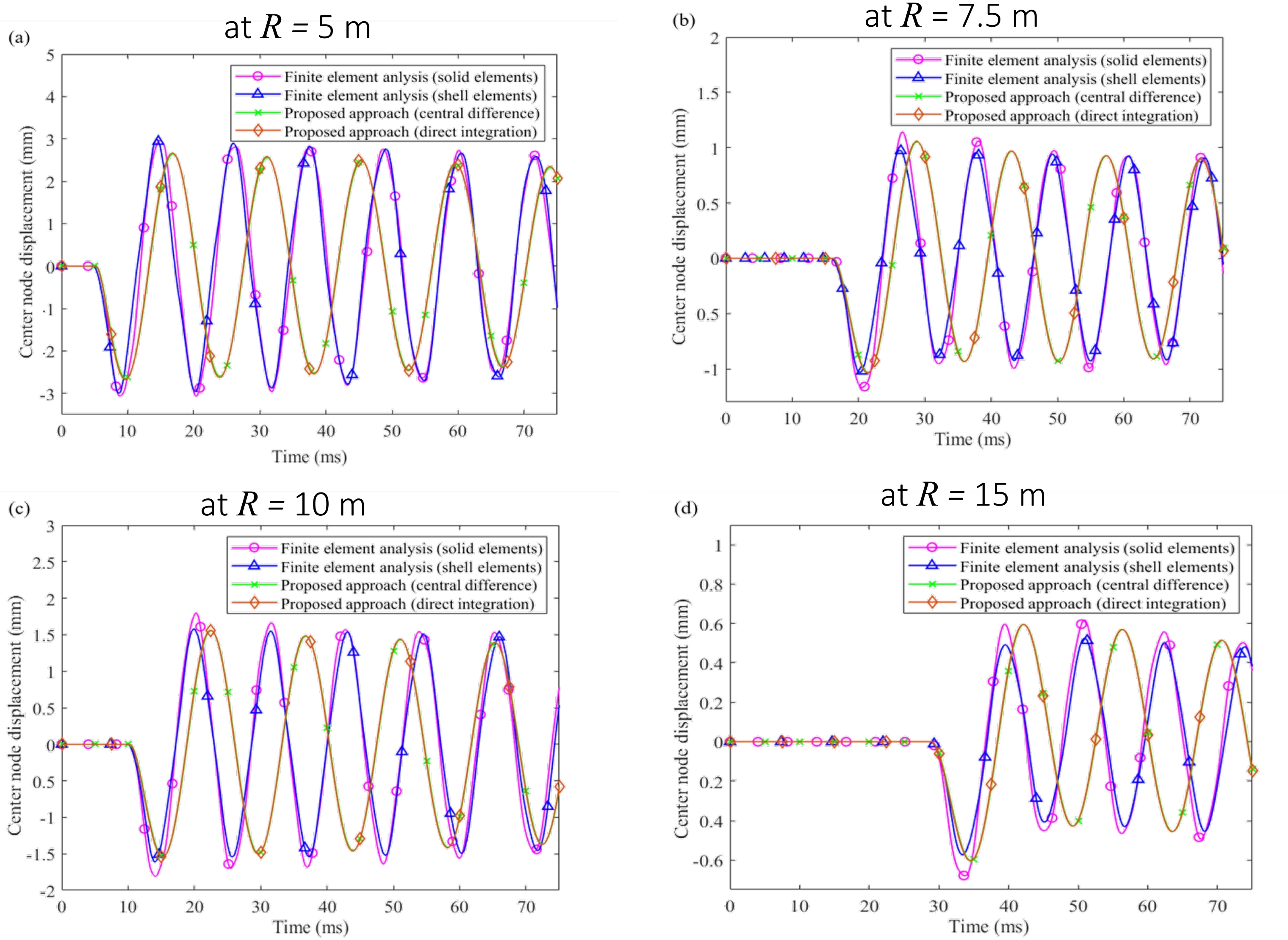

# FRP Composite Plates under Blast load

## Blast-induced response of concrete wall for varied materials properties and geometries FRP composite

### FRP Materials

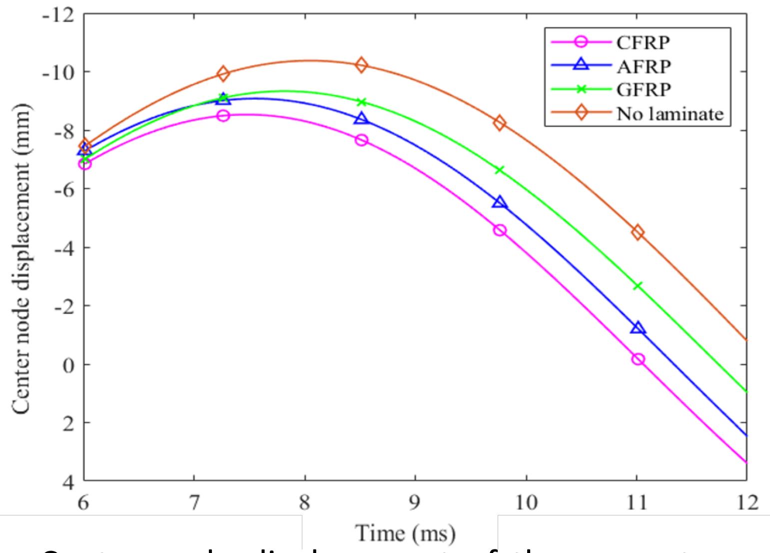


Center node displacement of the concrete wall with CFRP, AFRP, and GFRP laminates with configuration, (0°/90°/45°/-45°/0°/90°)$_s$.

### Stacking Sequence

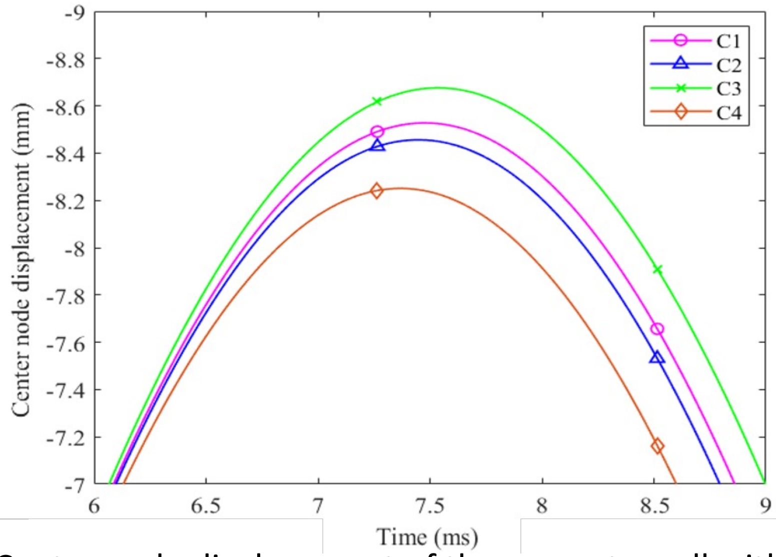


Center node displacement of the concrete wall with CFRP laminate with configurations,

C1 - (0°/90°/45°/-45°/0°/90°)$_s$
C2 - (0°/45°/-45°/90°/0°/45°)$_s$
C3 - (0°/90°/0°/90°/0°/90°)$_s$
C4 - (45°/-45°/45°/-45°/45°/-45°)$_s$.

### Number of Layers

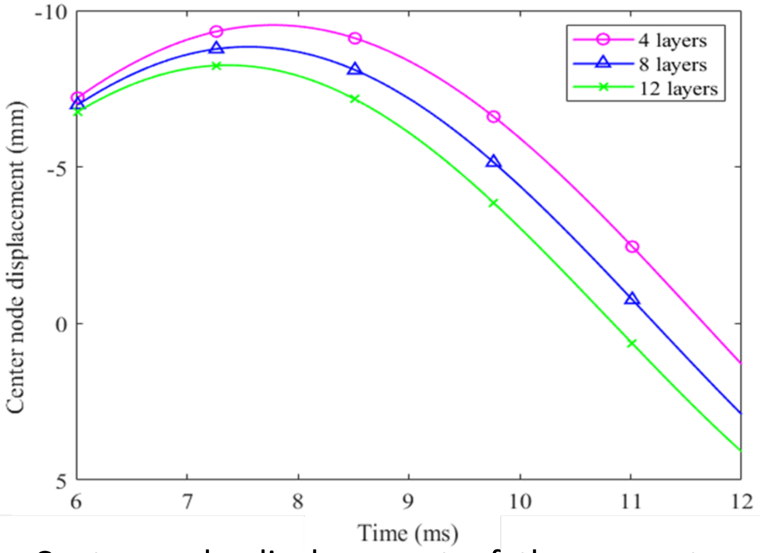


Center node displacement of the concrete wall with CFRP symmetric angle-ply laminate with varying number of lamina layers.

## Blast-induced response of RC walls for varied thickness and explosive weight

### Thickness of Concrete Wall

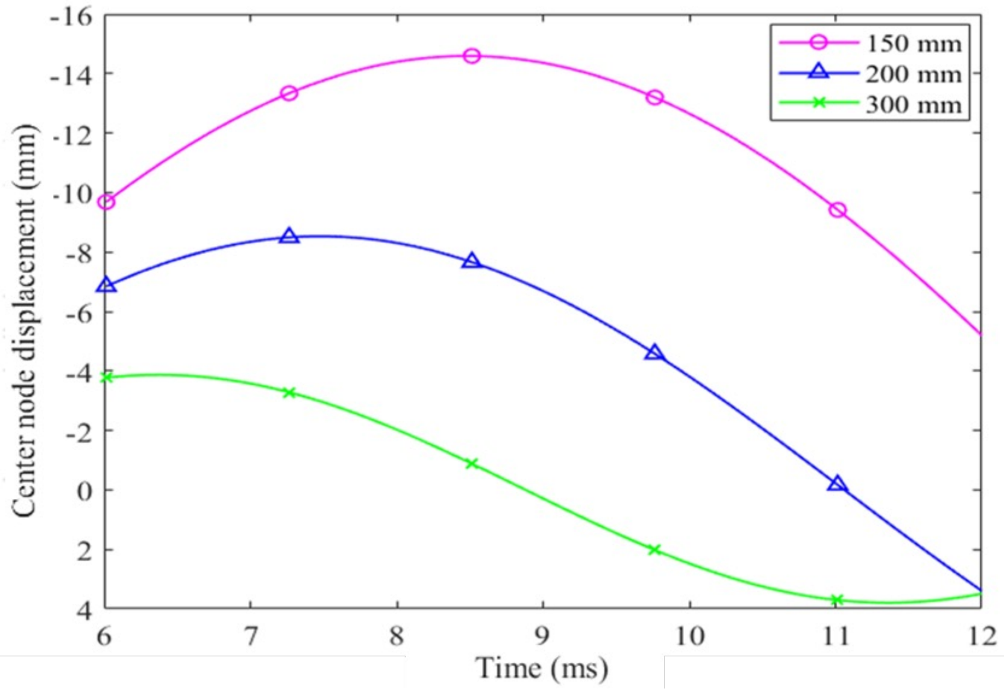


Center node displacement of the concrete wall with varied thicknesses.

### Weight of Explosive

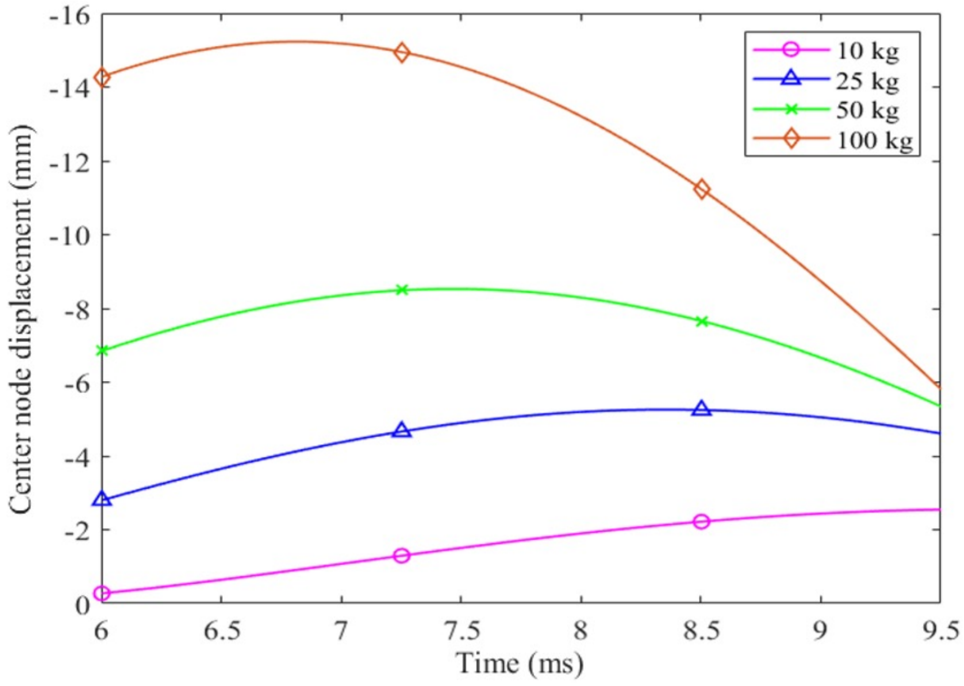


Center node displacement of the concrete wall with varied explosive weights.

## Different Failure Criteria and failure envelops

- Maximum Stress Failure Criterion

$$g = \max\left(\frac{\sigma_1}{X}, \frac{\sigma_2}{Y}, \frac{|\tau_{12}|}{S}\right)$$

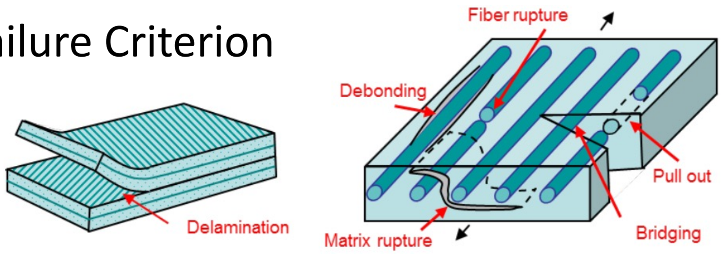


- Tsai-Hill Failure Criterion

$$g = \left(\frac{\sigma_1}{X}\right)^2 + \left(\frac{\sigma_2}{Y}\right)^2 - \left(\frac{\sigma_1\sigma_2}{X^2}\right) + \left(\frac{{\tau_{12}}^2}{S^2}\right)$$

Tsai-Wu Failure Criterion

$$g = \left(\frac{1}{X_t} - \frac{1}{X_c}\right)\sigma_1 + \left(\frac{1}{Y_t} - \frac{1}{Y_c}\right)\sigma_2 + \left(\frac{{\sigma_1}^2}{X_tX_c}\right) + \left(\frac{{\sigma_2}^2}{Y_tY_c}\right) - \left(\frac{\sigma_1\sigma_2}{\sqrt{X_tX_cY_tY_c}}\right) + \left(\frac{{\tau_{12}}^2}{S^2}\right)$$

(4) Hoffman Failure Criterion

$$g = \left(\frac{1}{X_t} - \frac{1}{X_c}\right)\sigma_1 + \left(\frac{1}{Y_t} - \frac{1}{Y_c}\right)\sigma_2 + \left(\frac{1}{X_tX_c}\right)\sigma_1^2 + \left(\frac{1}{Y_tY_c}\right)\sigma_2^2 - \left(\frac{1}{X_tX_c}\right)\sigma_1\sigma_2 + \left(\frac{\tau_{12}}{S}\right)^2$$

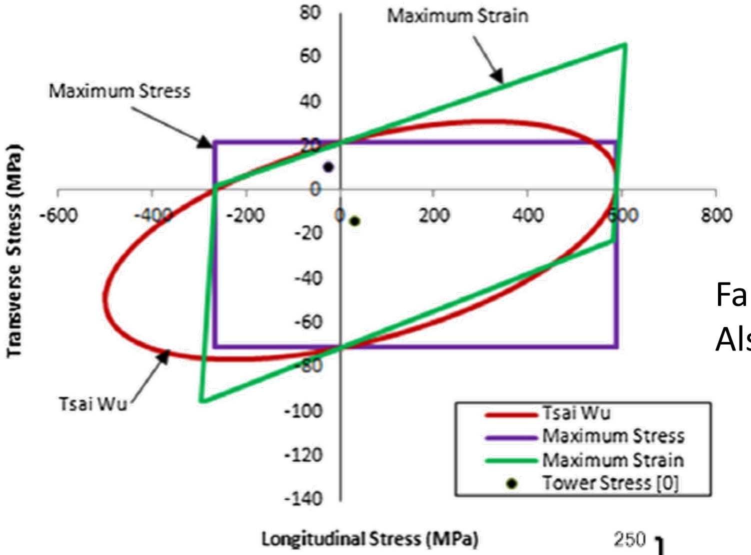


Failure envelopes for GFRP by Alshurafa et al. (2018)

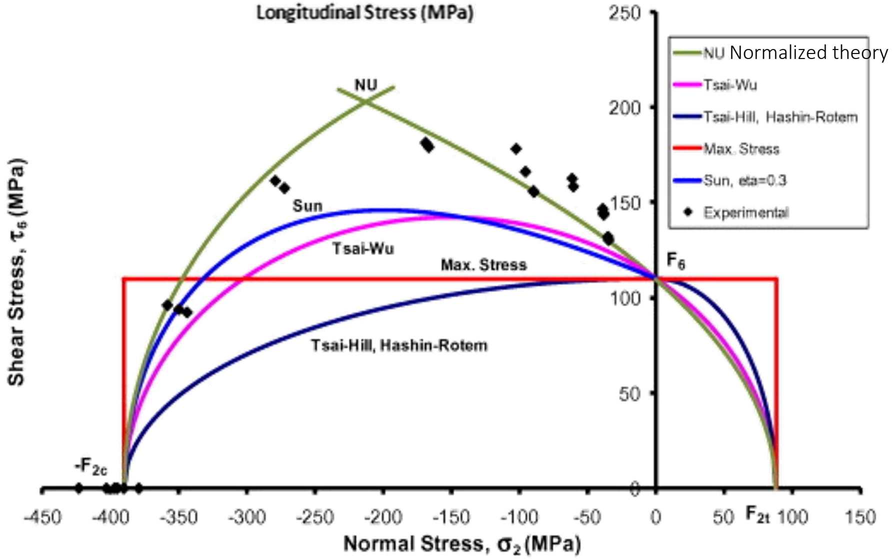


Failure envelopes of AS4/3501-6 CFRP composite under high rate transverse normal and shear stress by Daniel et al. (2011)

# Damage Evolution of FRP Composite Plates under Blast

## Damage evolution in FRP composite plate

- Hashin's Damage Failure Criterion

Fiber damage in tension ($\sigma_{11} \geq 0$)

$$(d_f^{\mathrm{T}})^2 = \left(\frac{\sigma_{11}}{X_{\mathrm{T}}}\right)^2 + \alpha\left(\frac{\tau_{12}}{S}\right)^2$$

Fiber damage in compression ($\sigma_{11} < 0$)

$$(d_f^{\mathrm{C}})^2 = \left(\frac{\sigma_{11}}{X_{\mathrm{C}}}\right)^2$$

Matrix damage in tension ($\sigma_{22} \geq 0$)

$$(d_m^{\mathrm{T}})^2 = \left(\frac{\sigma_{22}}{Y_{\mathrm{T}}}\right)^2 + \left(\frac{\tau_{12}}{S}\right)^2$$

Matrix damage in compression ($\sigma_{22} < 0$)

$$(d_m^{\mathrm{C}})^2 = \left(\frac{\sigma_{22}}{2S}\right)^2 + \left[\left(\frac{Y_{\mathrm{C}}}{2S}\right)^2 - 1\right]\left(\frac{\sigma_{22}}{Y_{\mathrm{C}}}\right) + \left(\frac{\tau_{12}}{S}\right)^2$$

Applied idealized blast load

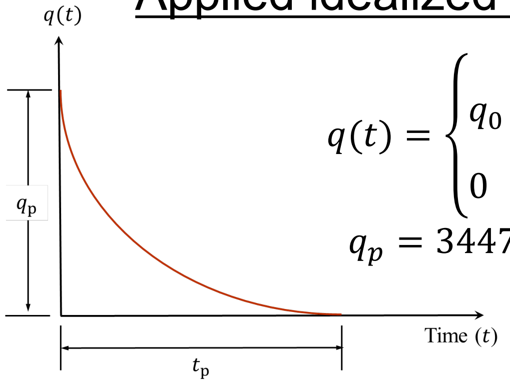


$$q(t) = \begin{cases} q_0\left(1 - \dfrac{t}{t_p}\right) e^{\frac{\alpha t}{t_p}} & \text{for } t \leq t_p \\ 0 & \text{for } t > t_p \end{cases}$$

$q_p$ = 3447 kPa, α = 2, $t_p$ = 0.1

$q_p$ = 3447 kPa, α = 2, $t_p$ = 0.1

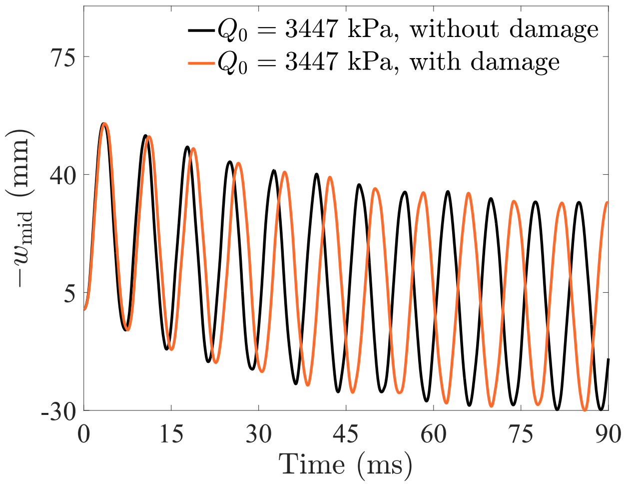


$q_p$ = 6894 kPa, α = 2, $t_p$ = 0.1 s

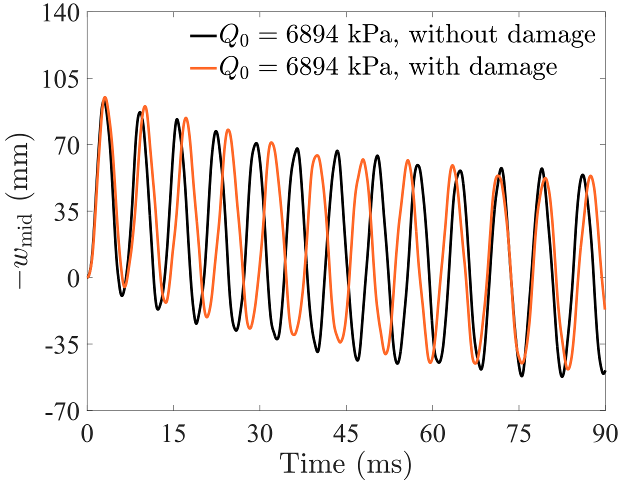


At time instant = 9 ms

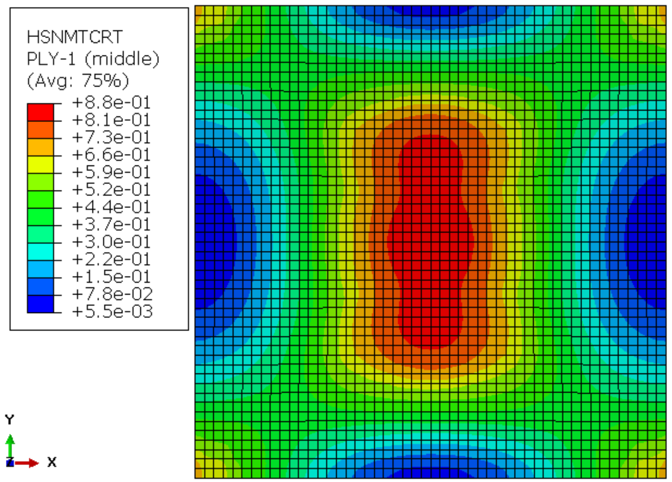


At time instant = 1.875 ms

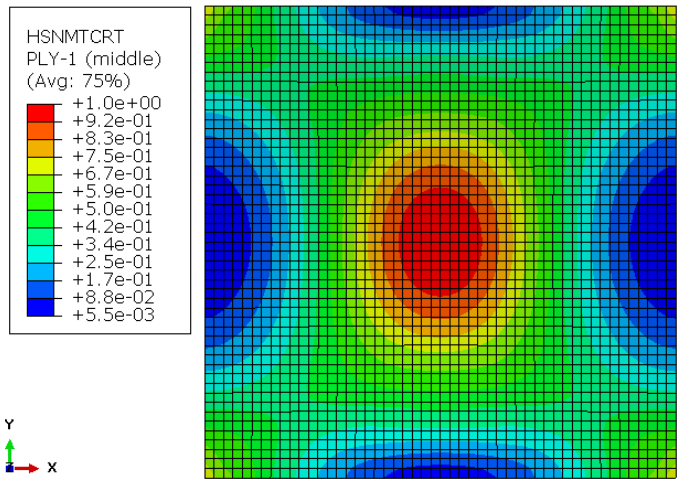

# FRP and Foam Sandwich Composite under

## Deformation shapes of sandwich panels for $W$ = 2.5 kg and $R$ = 1 m

Time instant = 2.17 ms　　Time instant = 3.09 ms　　Time instant = 5.26 ms

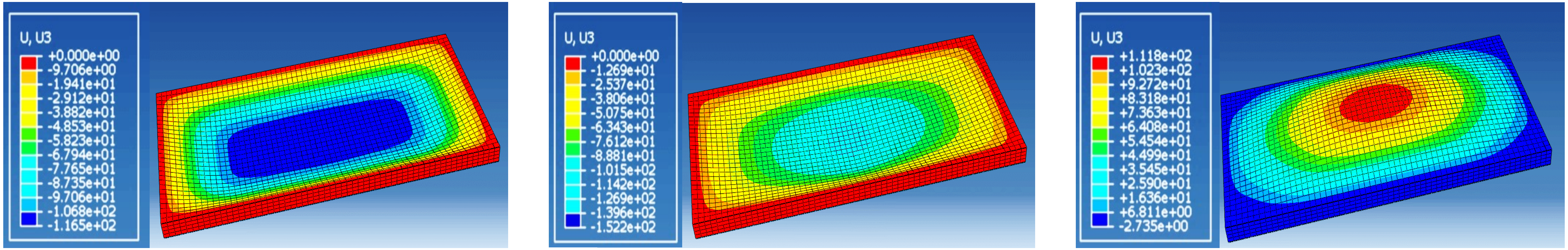


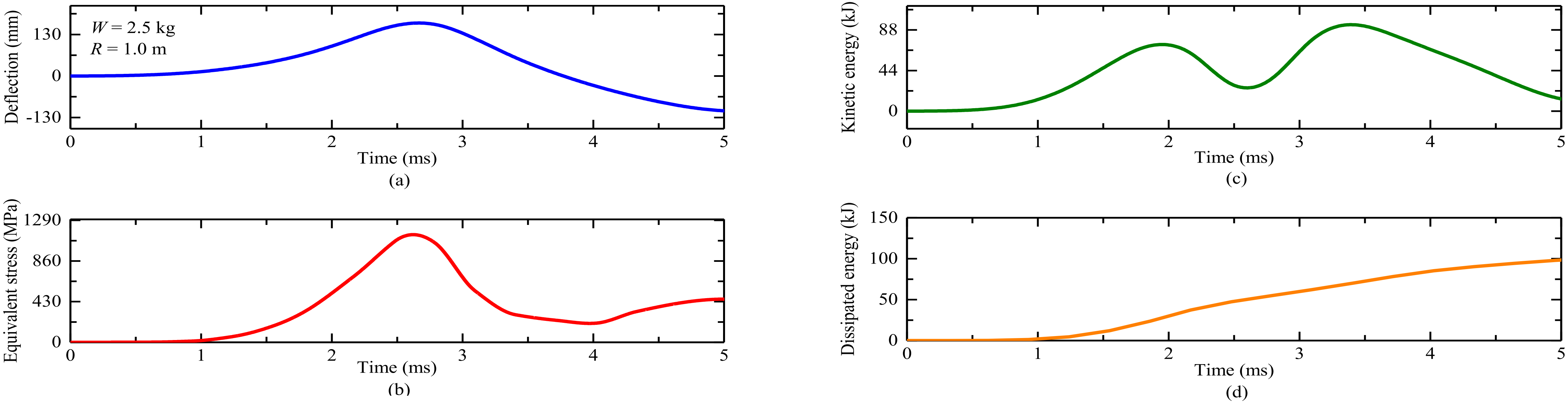

# Basalt Fiber Reinforced Polymer (BFRP)

## Experimental Investigations on BFRP-Beams

### Prestressing Application

- Already developed anchors are used.
- Hollow load cells are used.
- 5-mm strain gauges.

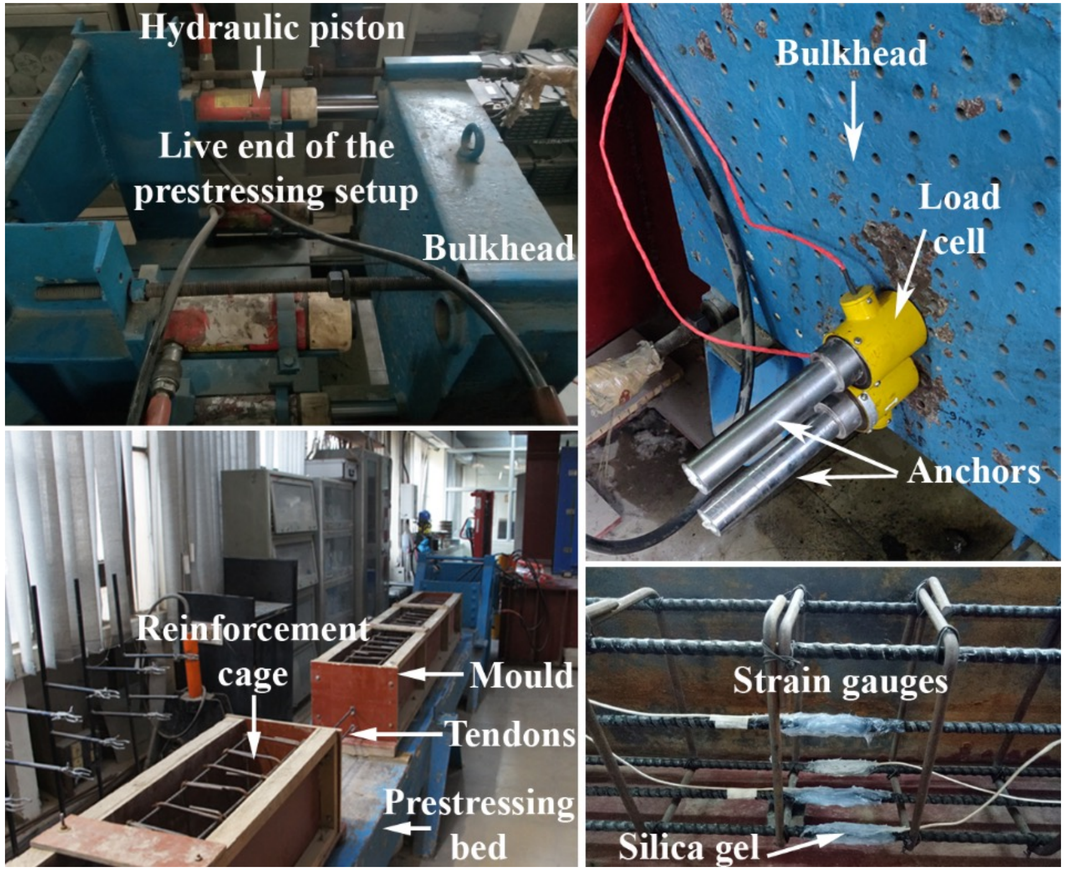


### Construction of Beams

- Three different grades of concrete are used.

## Four-Point Bending Test on Beams

- Beams are instrumented and tested.
- The instrumentation includes the use of:

1. load cell,
2. strain gauges,
3. crack transducer, and
4. linear variable differential transformer (LVDT).

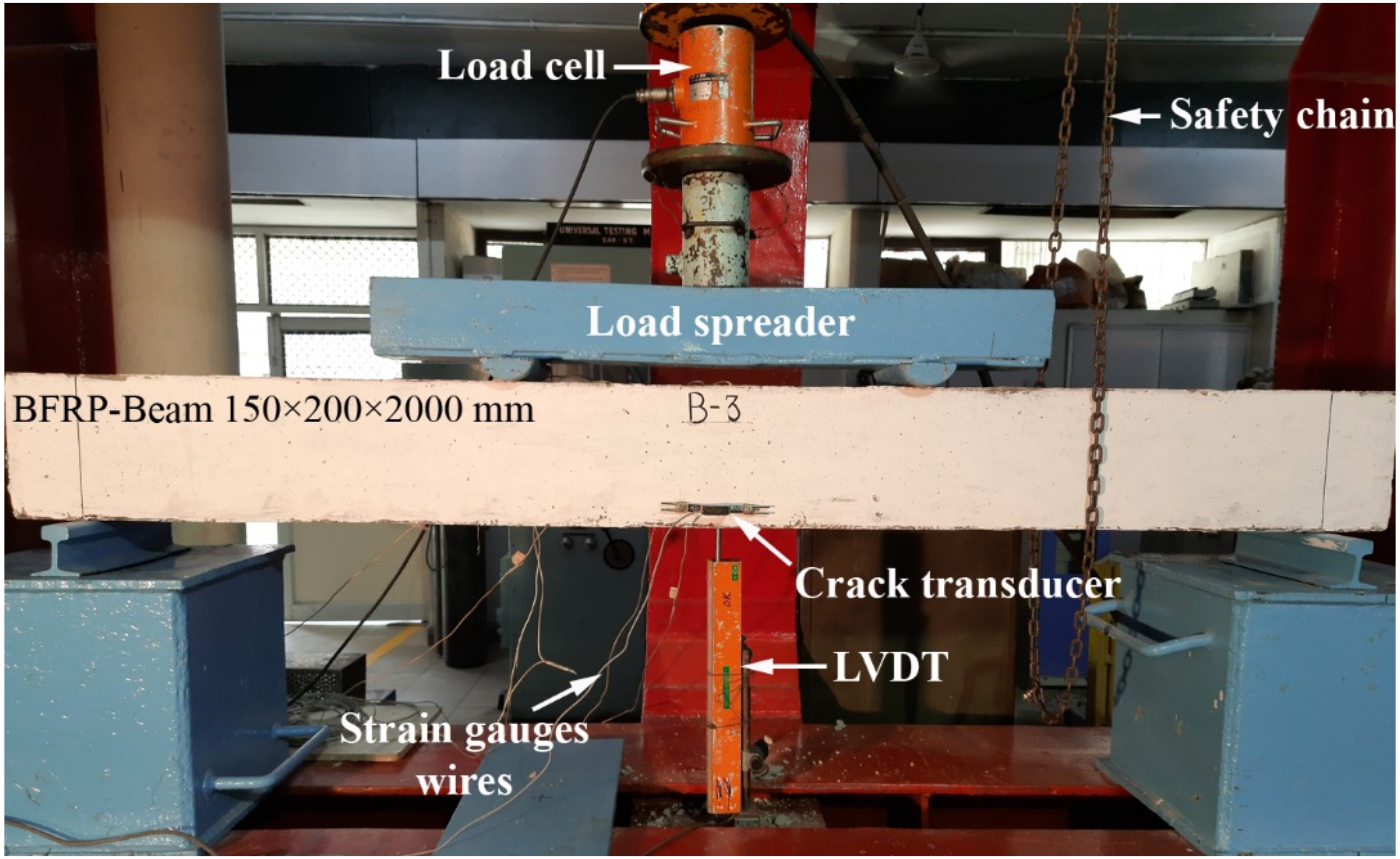

# Experimental Investigations on BFRP-Beams: Experimental Results

## Failure Mode and Crack Pattern

- Failure of beams in Series 1 and 2: crushing of concrete.
- Failure of beams in Series 3 and 4: rupturing of BFRP rebars/ tendons.
- Beams in Series 1, 2, and 3: excessive cracking, which is desirable,
- Beams of Series 4: extremely few numbers of cracks.

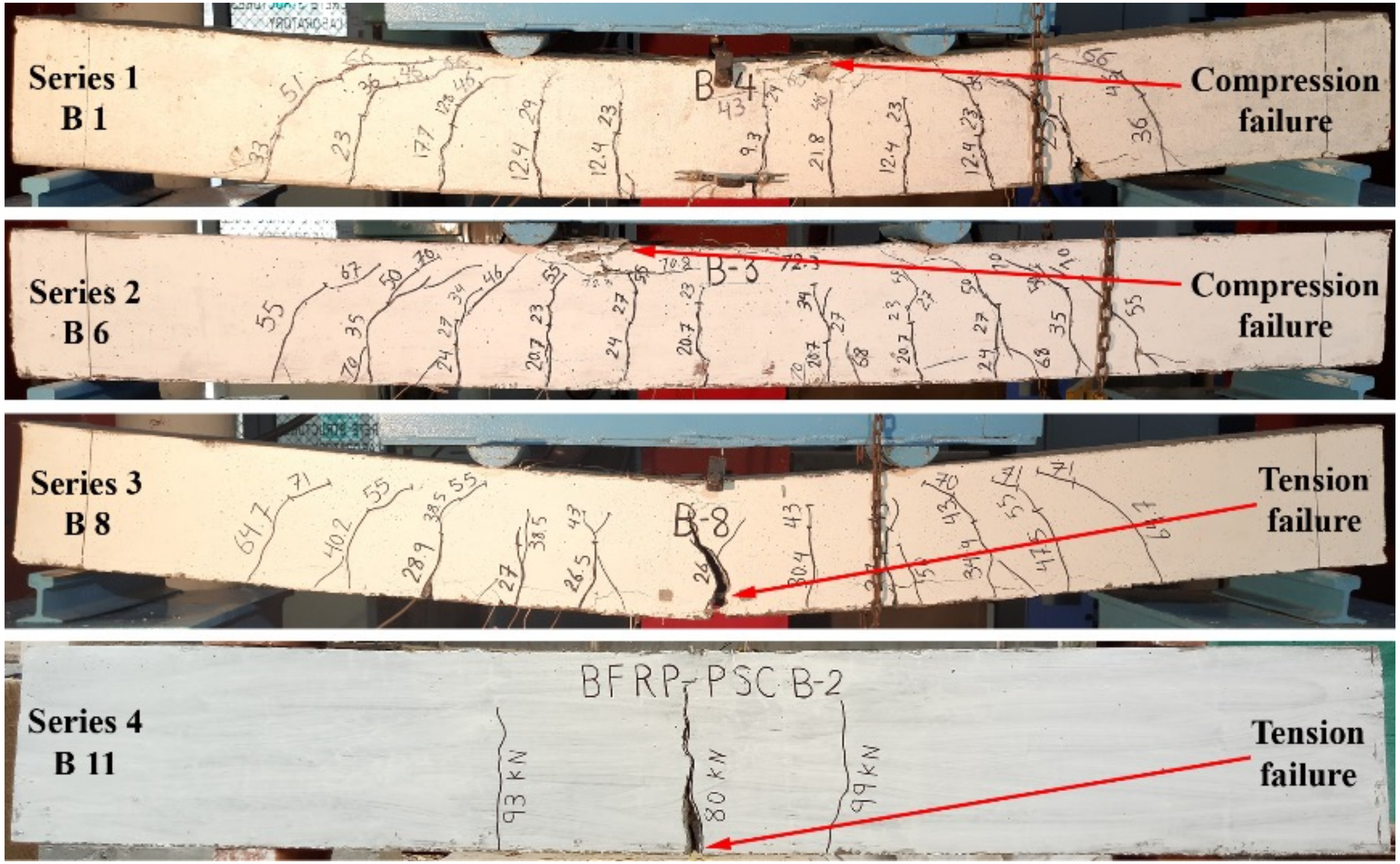

## Flexural Analysis of BFRP-Beams: Finite Element Analysis (FEA)

- Concrete is modeled as 8-node linear brick elements (C3D8R).
- FRP bars are modeled using 2-node linear truss elements (T3D2).
- The mesh size is set to 30 mm.
- The analysis is run in static step up to failure.

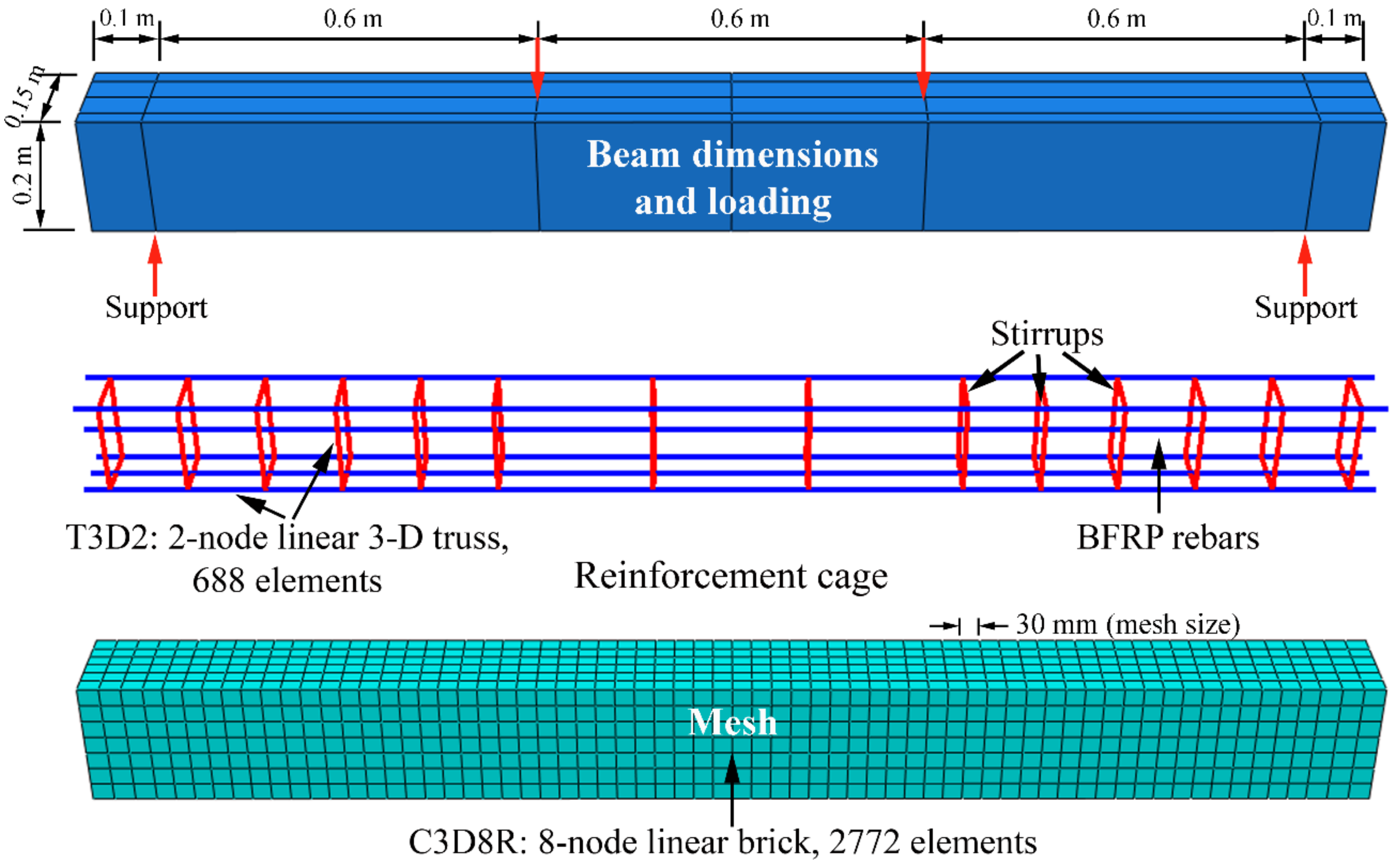

## Flexural Analysis of BFRP-Beams: FEA results

- Compression-controlled failure in Series 1 and tension-controlled failure in Series 3.

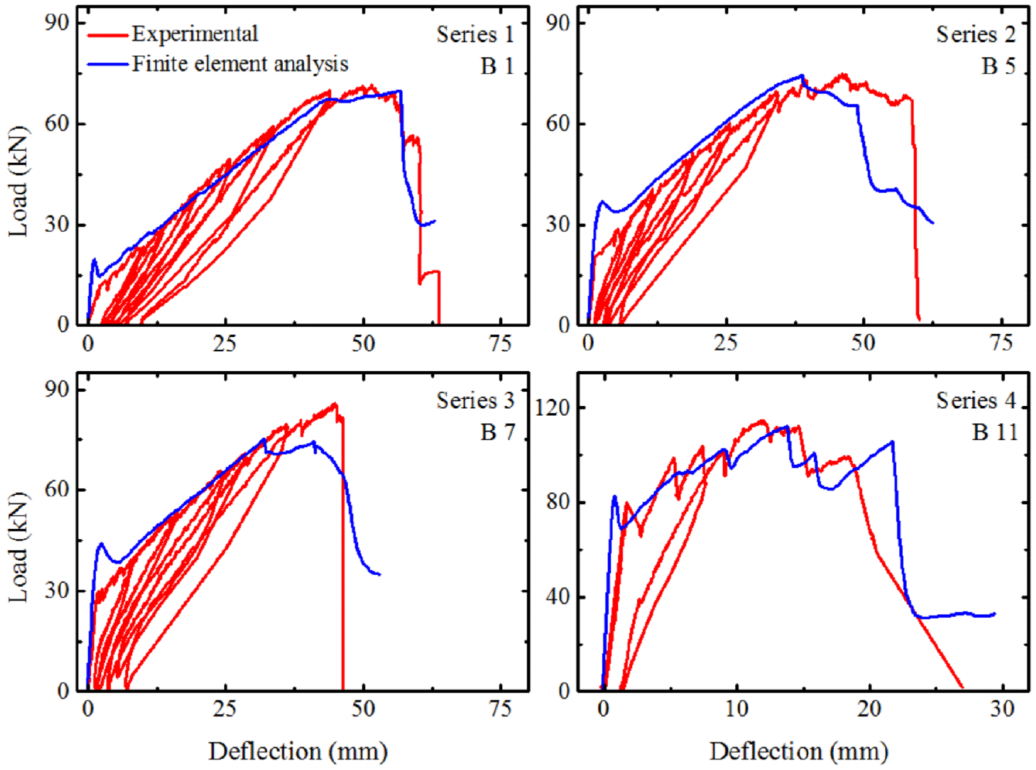


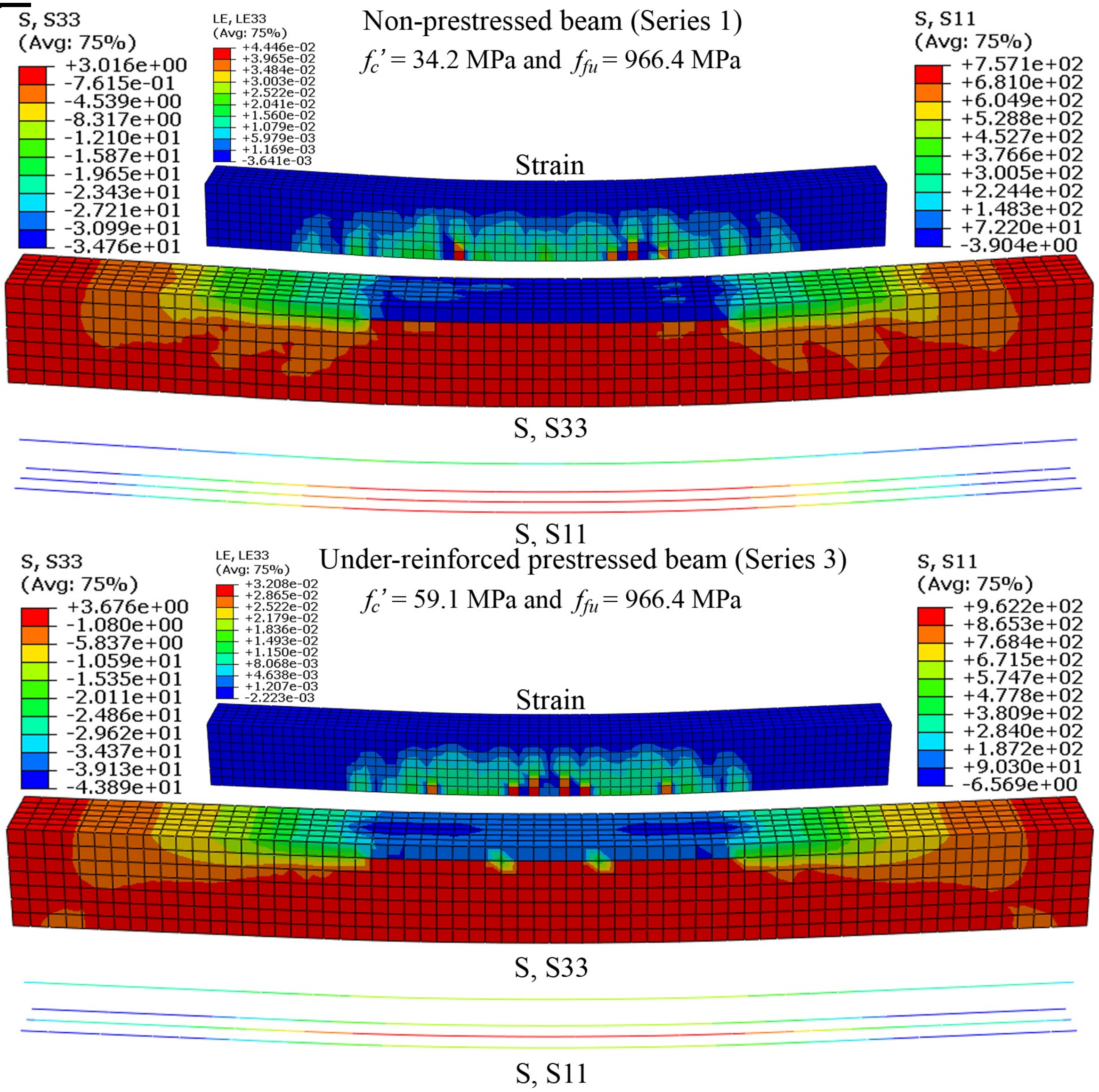


**The FEA results are in a good agreement with the experimental findings.**

# Reinforced Concrete (RC) Panel with BFRP Rods

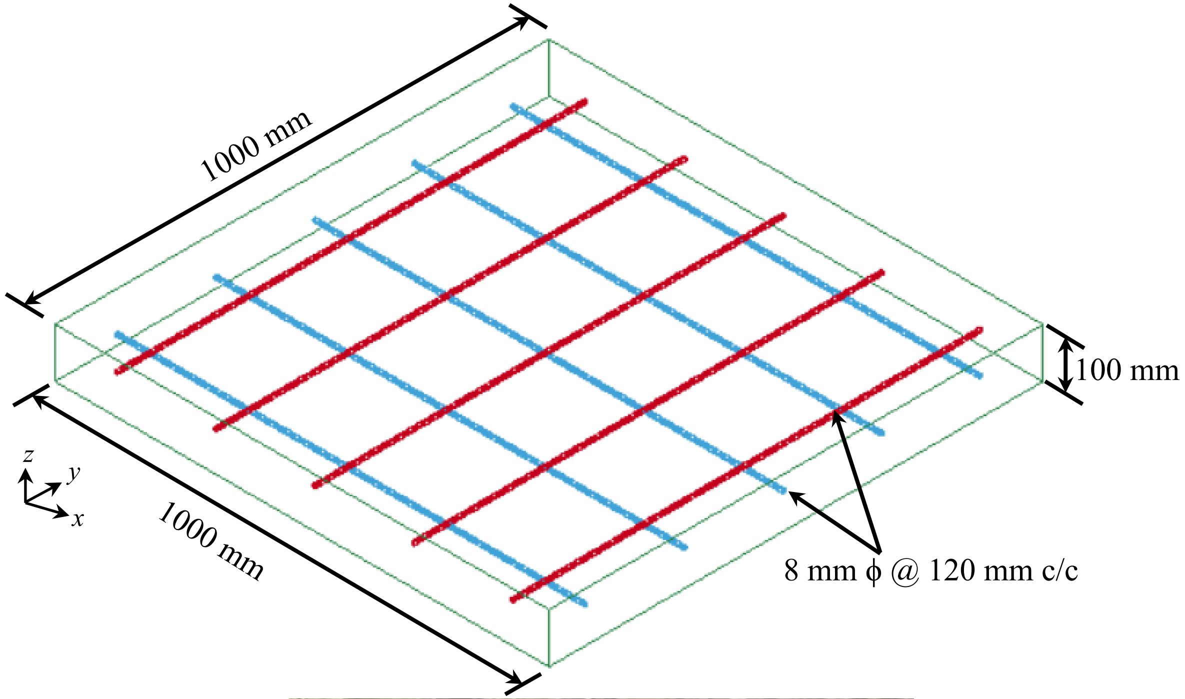


- **Dimensions of Panel:** 1 m × 1 m × 0.1 m
- **Reinforcement:** Basalt fiber reinforced polymer (BFRP)
- **Diameter of reinforcement:** 8 mm
- **Location of reinforcement:** Distance of 50 mm from top of the panel (in depth direction) and at a distance of 200 mm center to center with concrete cover of 30 mm
- **Grade of Concrete:** M50
- **Boundary condition:** Simply supported on all four corners
- **Blast type:** Contact blast
- **Explosive type:** TNT

# Reinforced Concrete (RC) Panel with BFRP Rods

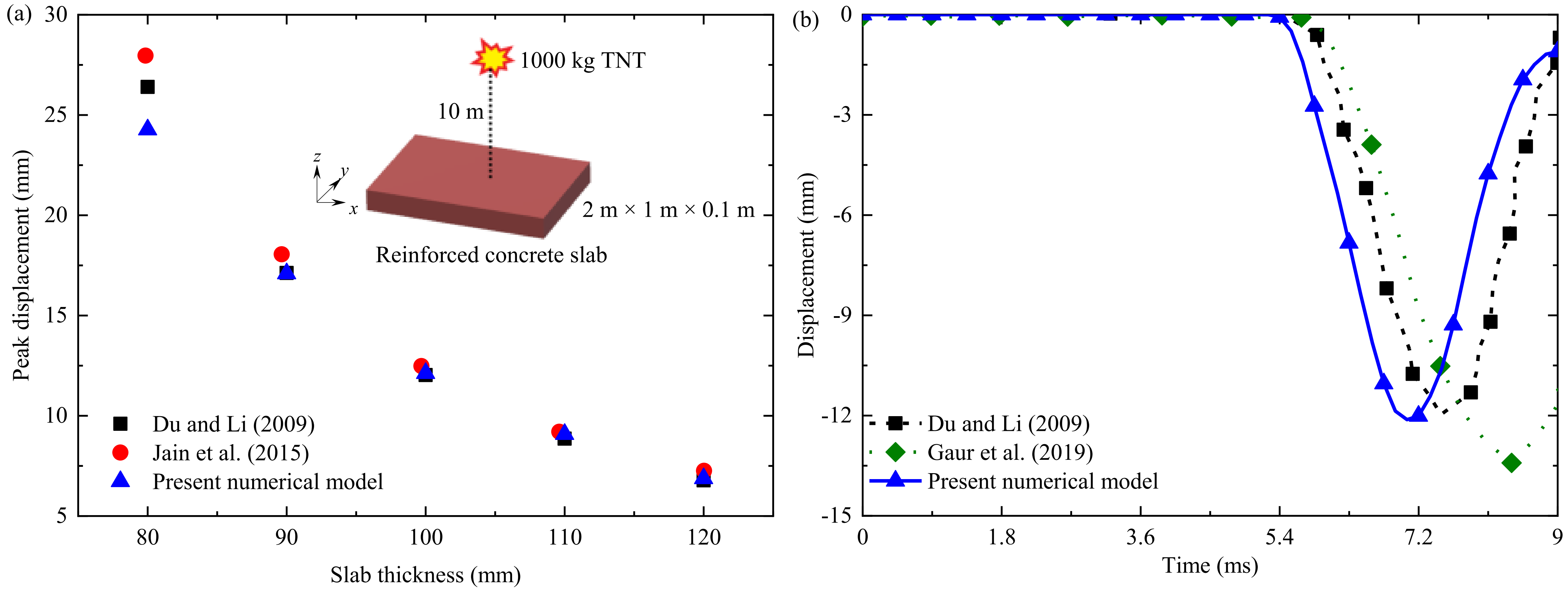


Numerical simulation in LS-DYNA® and the results reported by (a) Du and Li (2009); Jain et al. (2015), and (b) Gaur et al. (2019) for peak displacement values considering different slab thickness and displacement time history

# Reinforced Concrete (RC) Panel with BFRP Rods

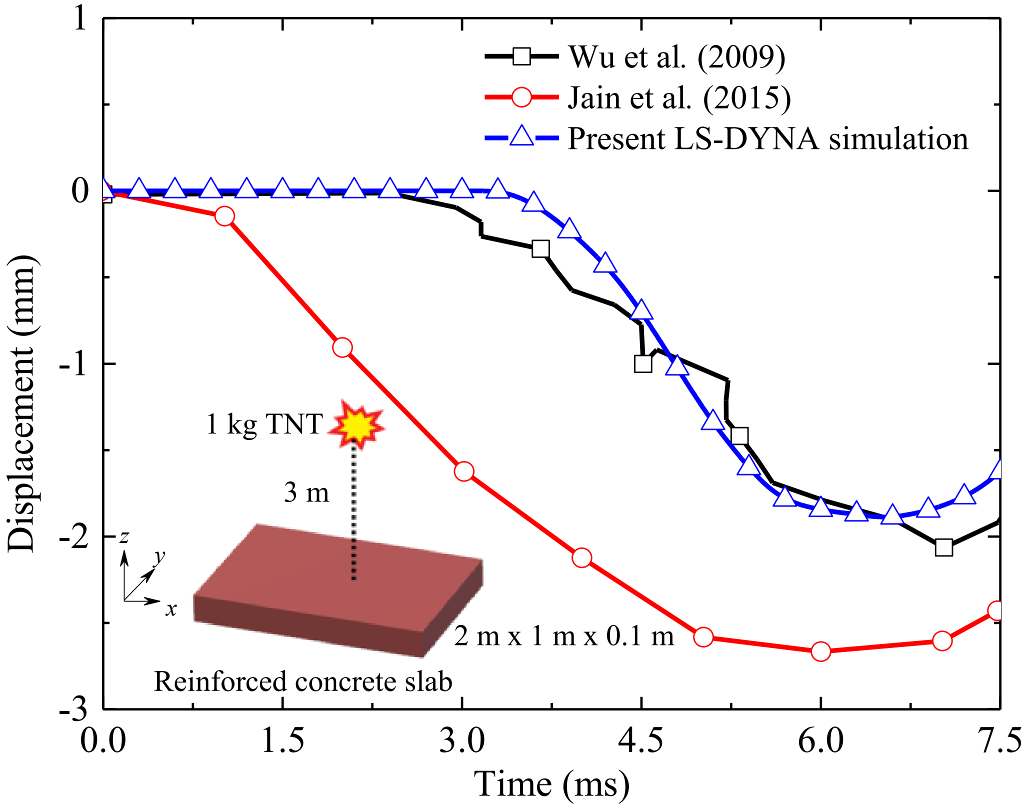


Displacement time history between present LS-DYNA® simulation and the results reported by Wu et al. (2009) and Jain et al. (2015)

Peak reflected and incident pressure between studies reported by Wu et al. (2009), UFC-3-340-02 (2008), and values obtained by LS-DYNA® simulation

| Particulars | Peak reflected pressure values (MPa) | Peak incident pressure values (MPa) |
|---|---|---|
| **Wu et al. (2009)** | 0.3 | Not reported |
| **UFC-3-340-02 (2008)** | 0.32 | 0.119 |
| **Present LS-DYNA® simulation** | 0.33 | 0.118 |

# Reinforced Concrete (RC) Panel with BFRP Rods

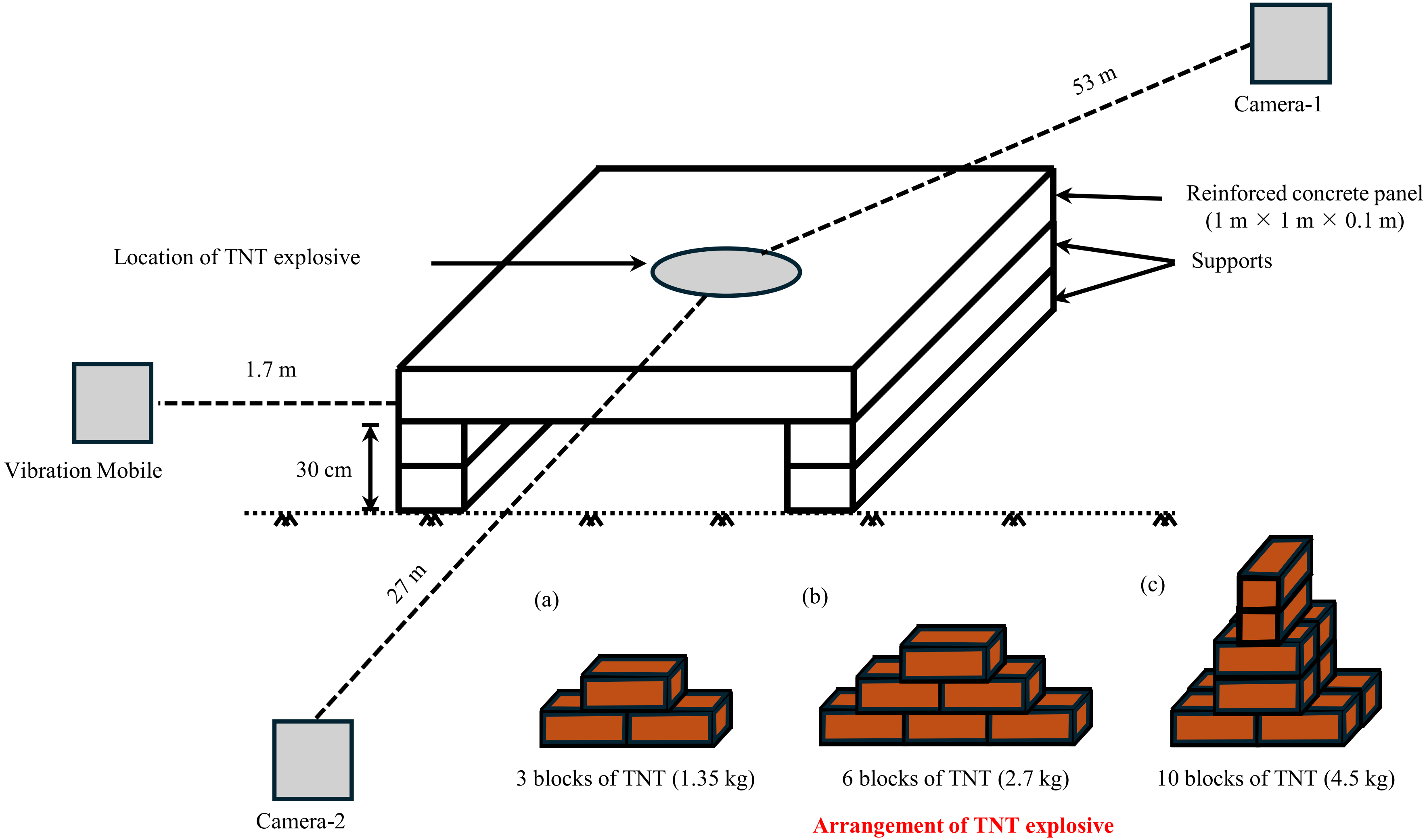


Position of camera, vibration mobile, and TNT explosive during the field test

# Reinforced Concrete (RC) Panel with BFRP Rods

Field test of BFRP reinforced concrete (RC) panel subjected to 1.35 kg TNT charge weight under contact blast

# Reinforced Concrete (RC) Panel with BFRP Rods

Field test of BFRP reinforced concrete (RC) panel subjected to 4.5 kg TNT charge weight under contact blast

# Reinforced Concrete (RC) Panel with BFRP Rods

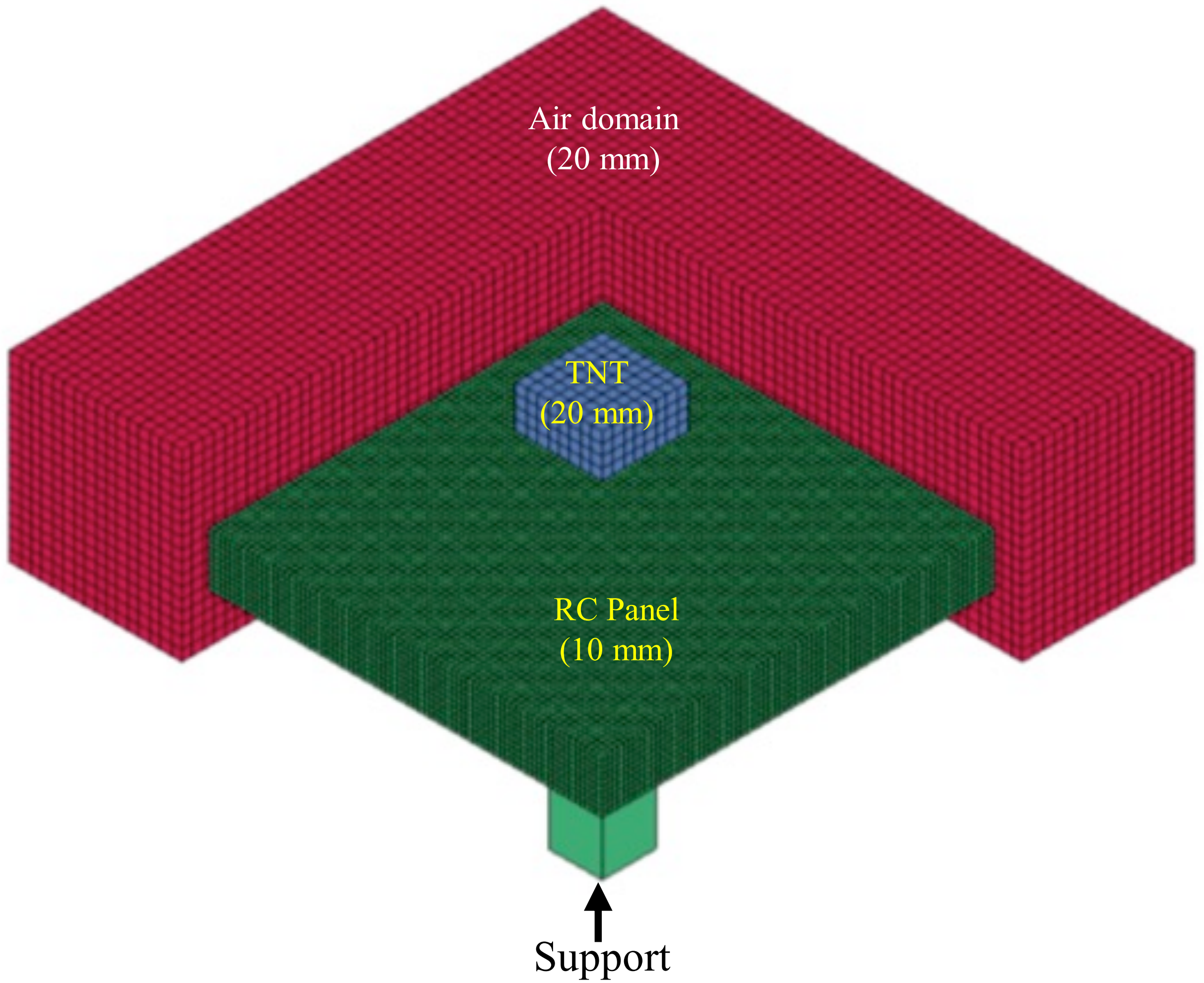


Finite element model prepared in LS-DYNA® for contact blast type simulation

| Entity | | Material model |
|---|---|---|
| Concrete | | Johnson-Holmquist concrete (MAT_111) and Concrete damage (MAT_72R3) |
| Reinforcement bars | BFRP | Piecewise linear plasticity (MAT_024) |
| | Steel | Plastic kinematic (MAT_003) |
| TNT | | High explosive burn (MAT_008) |
| Air | | Null (MAT_009) |

# Reinforced Concrete (RC) Panel with BFRP Rods

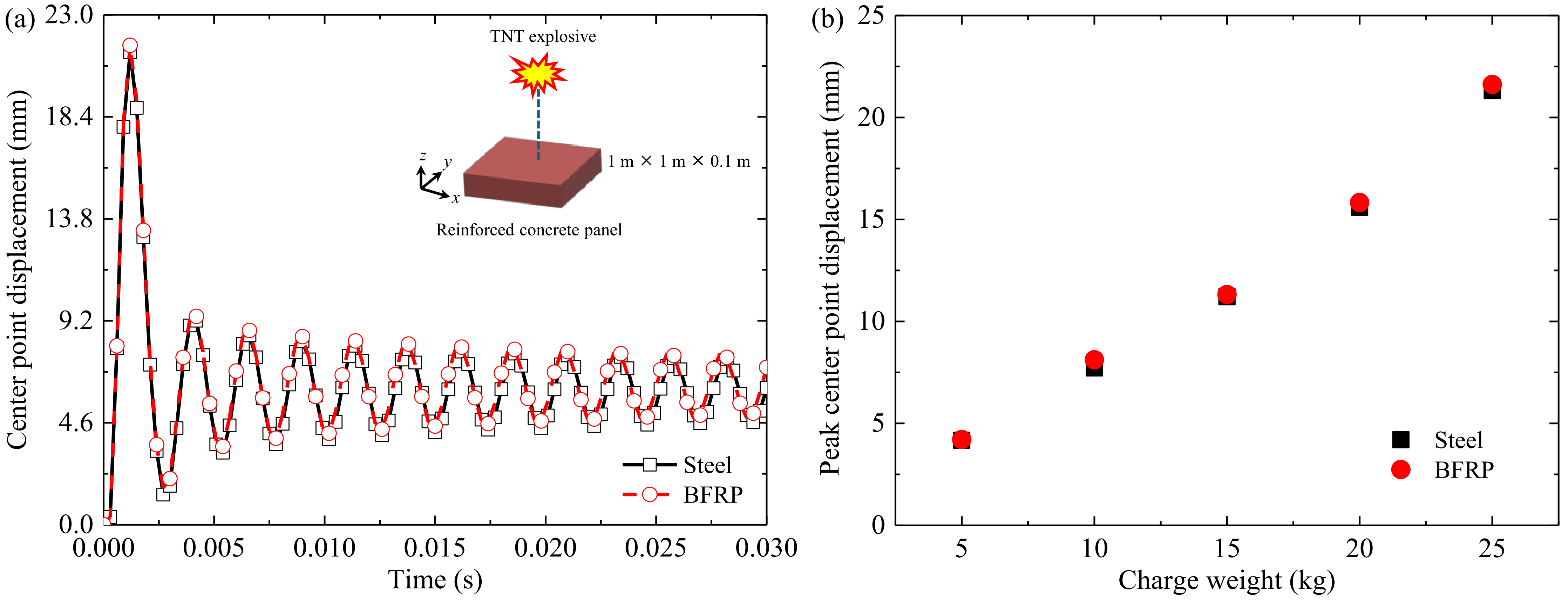


Steel- and BFRP-reinforced concrete panel (a) displacement time history (b) peak center point displacement

# Reinforced Concrete (RC) Panel with BFRP Rods

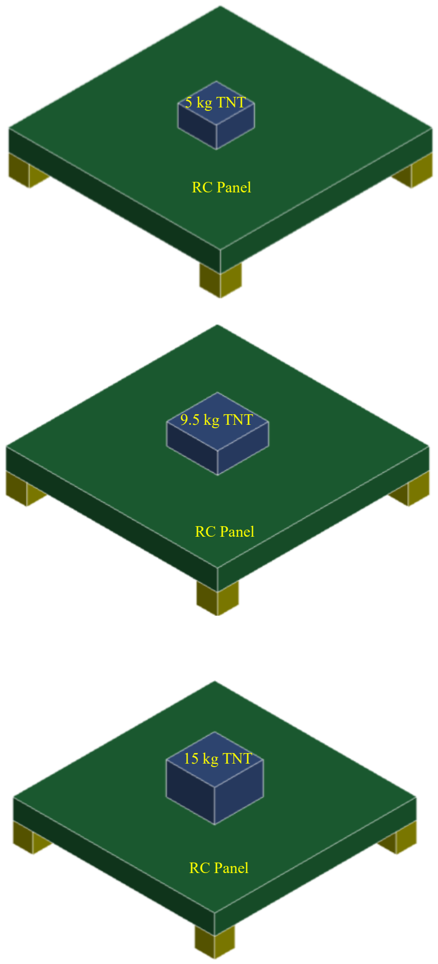


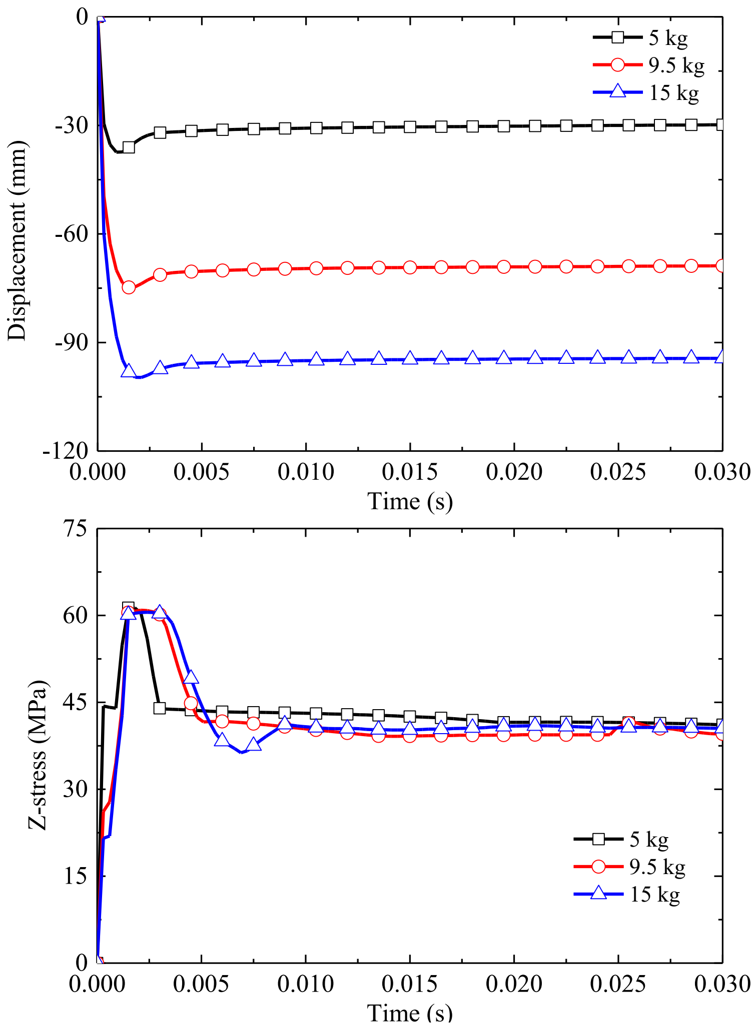


Finite element (FE) model of RC panel along with TNT explosive of three different charge weight

Displacement and *z*-stress time history of RC panel corresponding to different charge weights

# Reinforced Concrete (RC) Panel with BFRP Rods

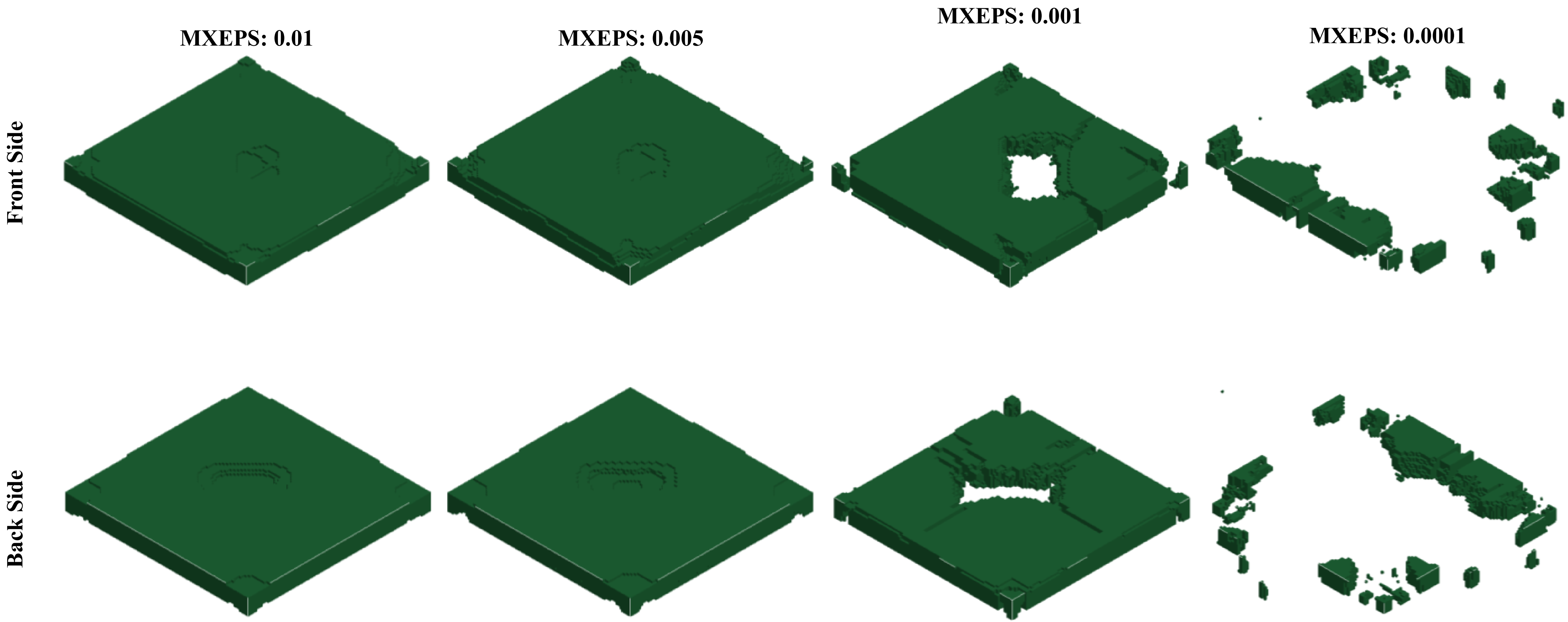


Damaged state of RC panel (front and back side) at $t$ = 0.02 s for four different principal strains

# Reinforced Concrete (RC) Panel with BFRP Rods

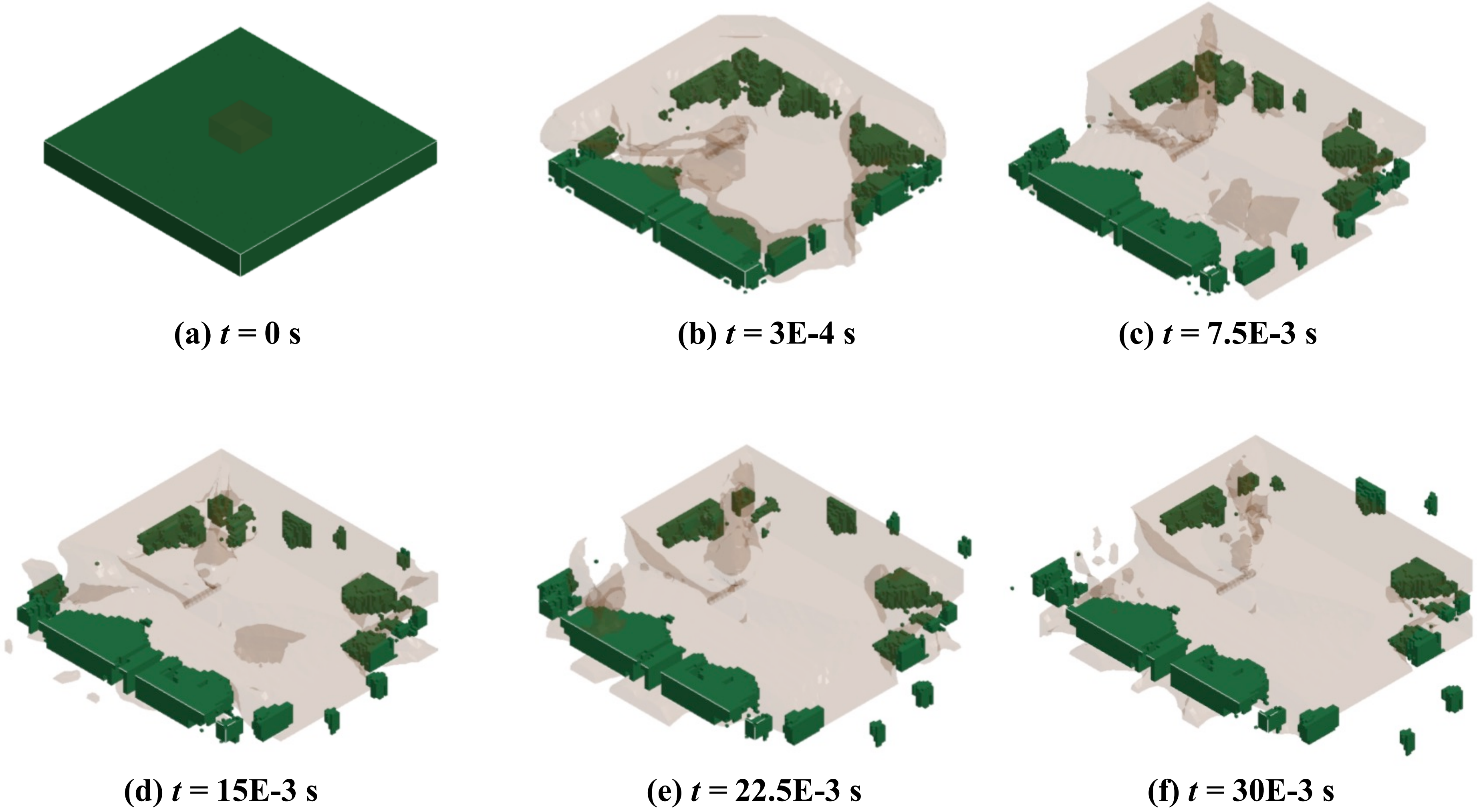


Blast wave propagation at different time interval for the panel subjected to 3 kg TNT blast load

# Reinforced Concrete (RC) Panel with BFRP Rods

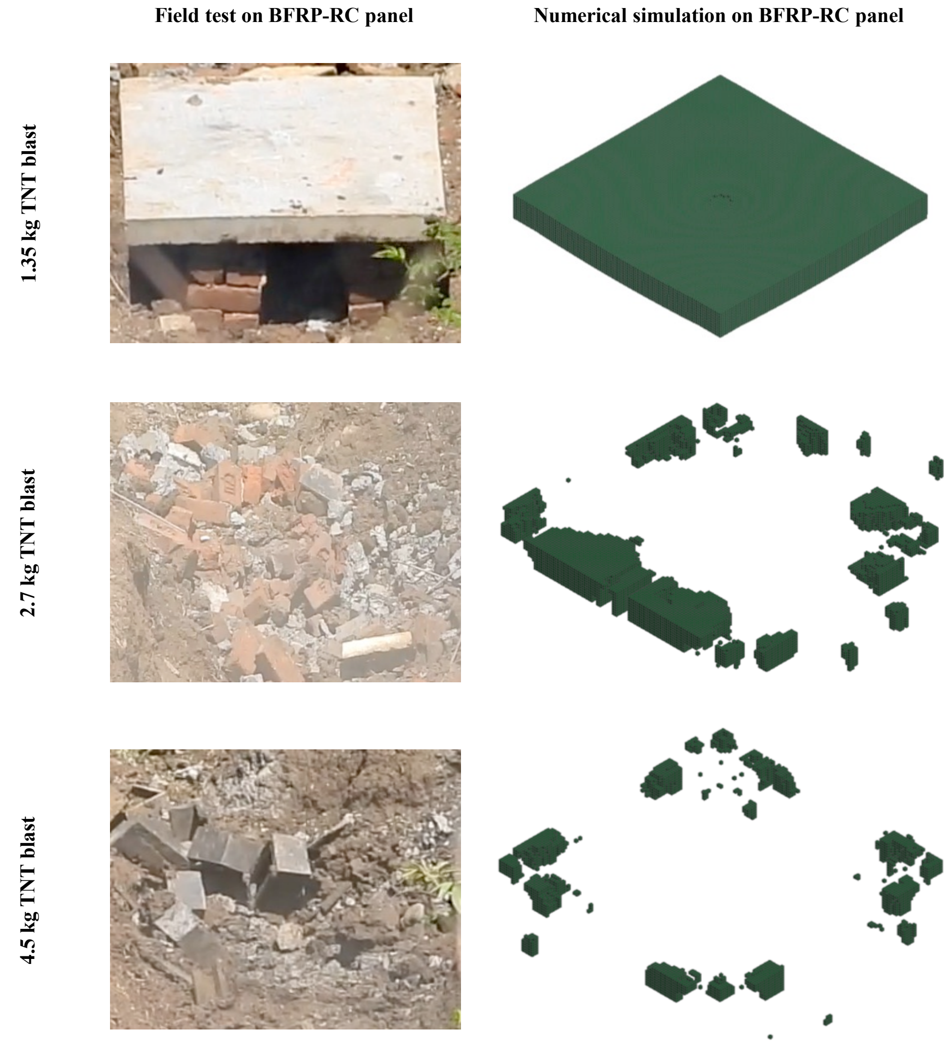


Damaged state of BFRP-RC panel subjected to different blast loads in case of field test and numerical simulation

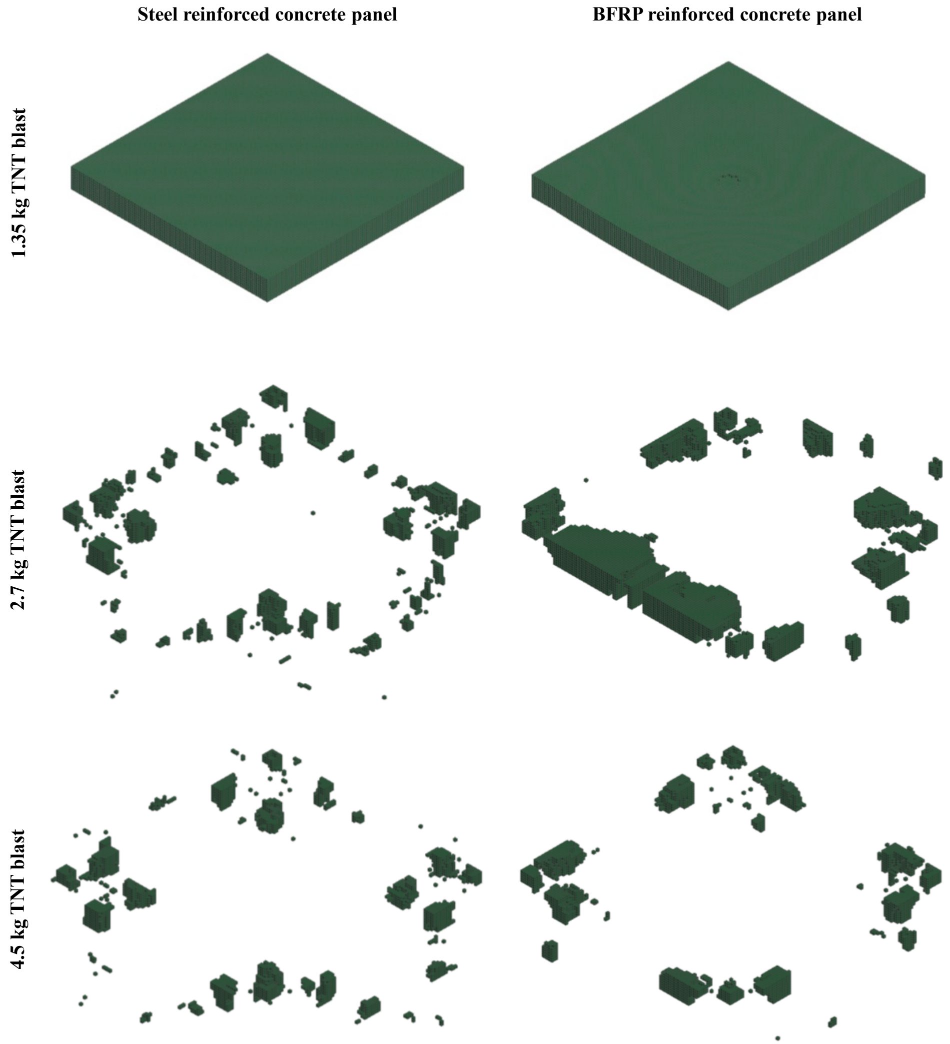


Damaged state of RC panel subjected to different blast loads for steel- and BFRP RC panels

# Reinforced Concrete (RC) Panel with BFRP Rods

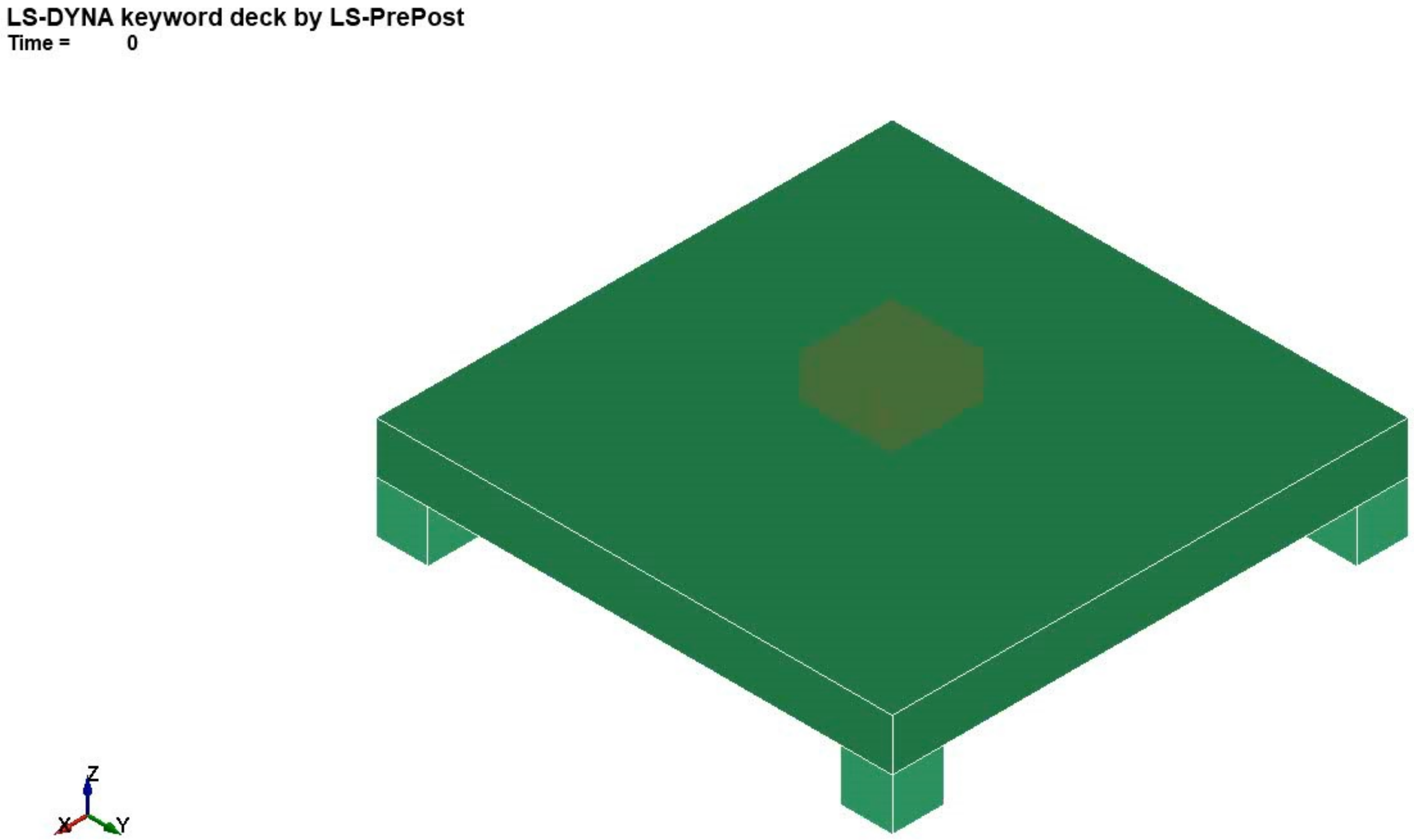


BFRP reinforced concrete panel subjected to 4.5 kg TNT charge weight

# Prestressed Concrete (PSC) Wall with BFRP Strands

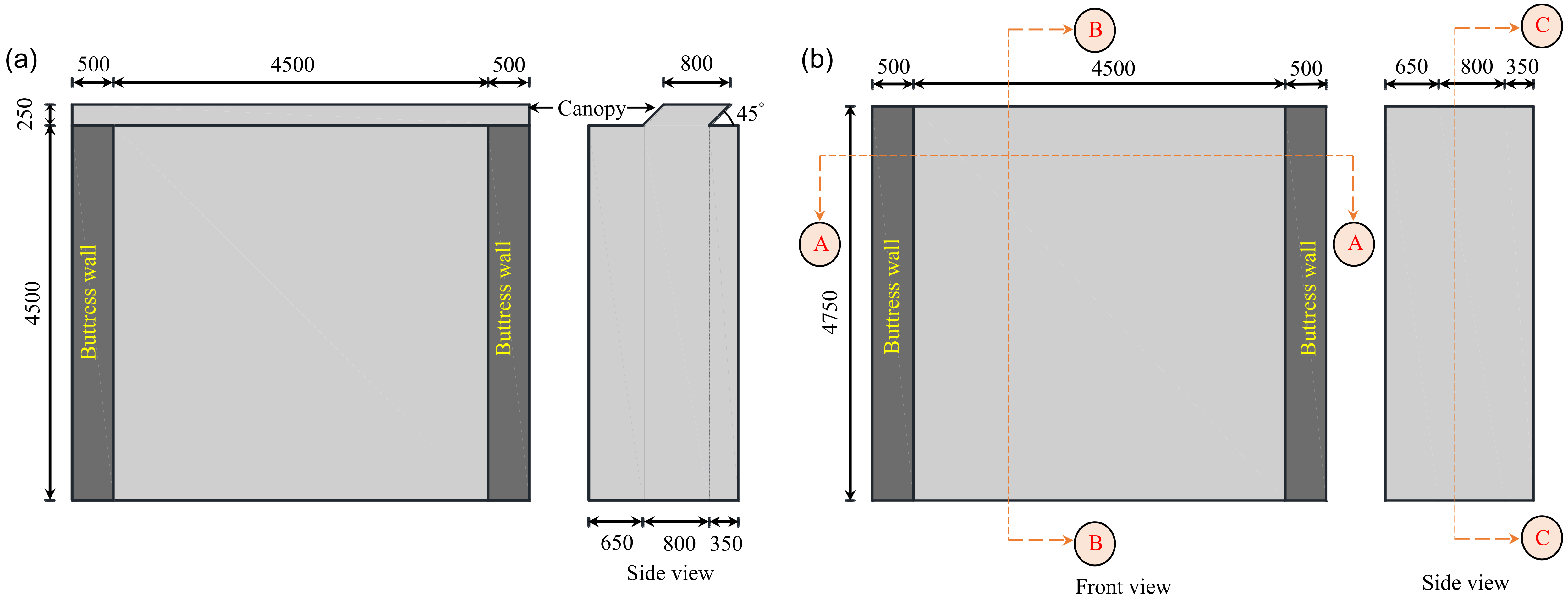


Dimensions of the prestressed concrete (PSC) wall (a) original (b) blast/impact retrofit

# Prestressed Concrete (PSC) Wall with BFRP Strands

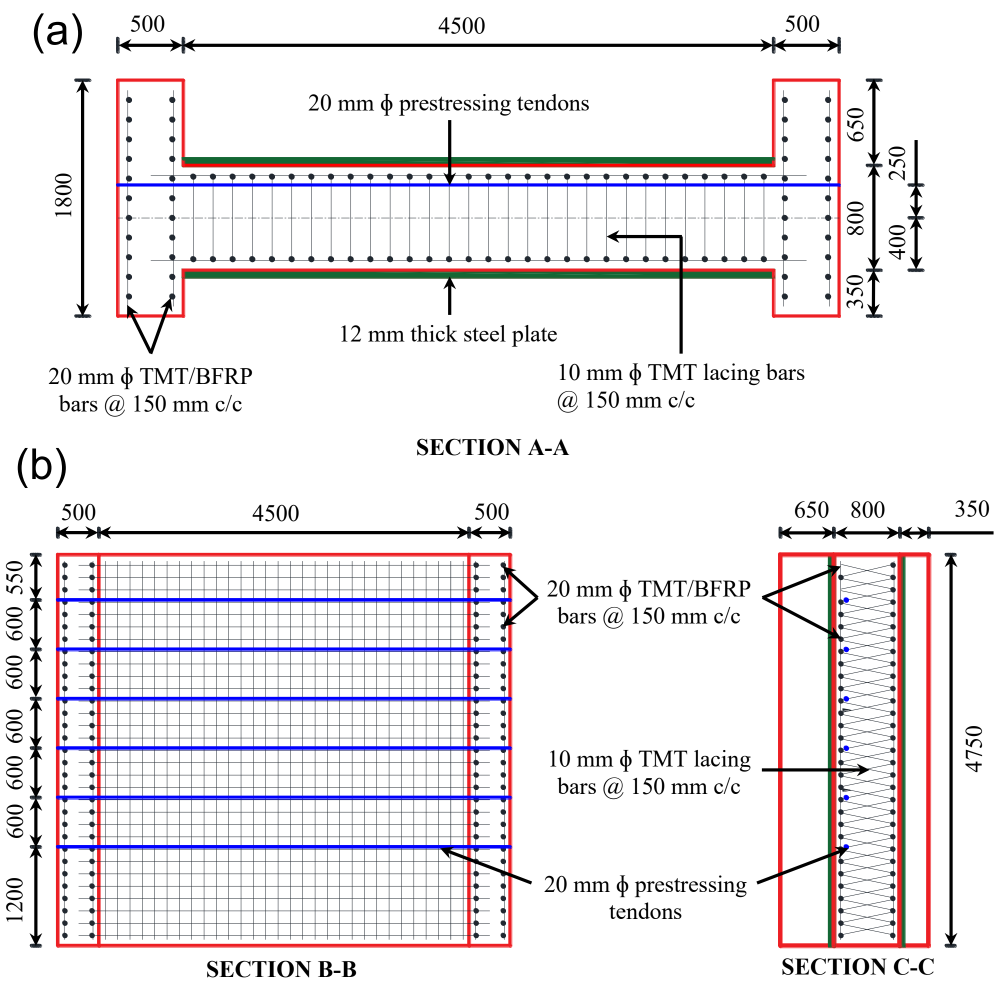


Section of the reinforced concrete (RC) wall (a) top view (b) front and side view

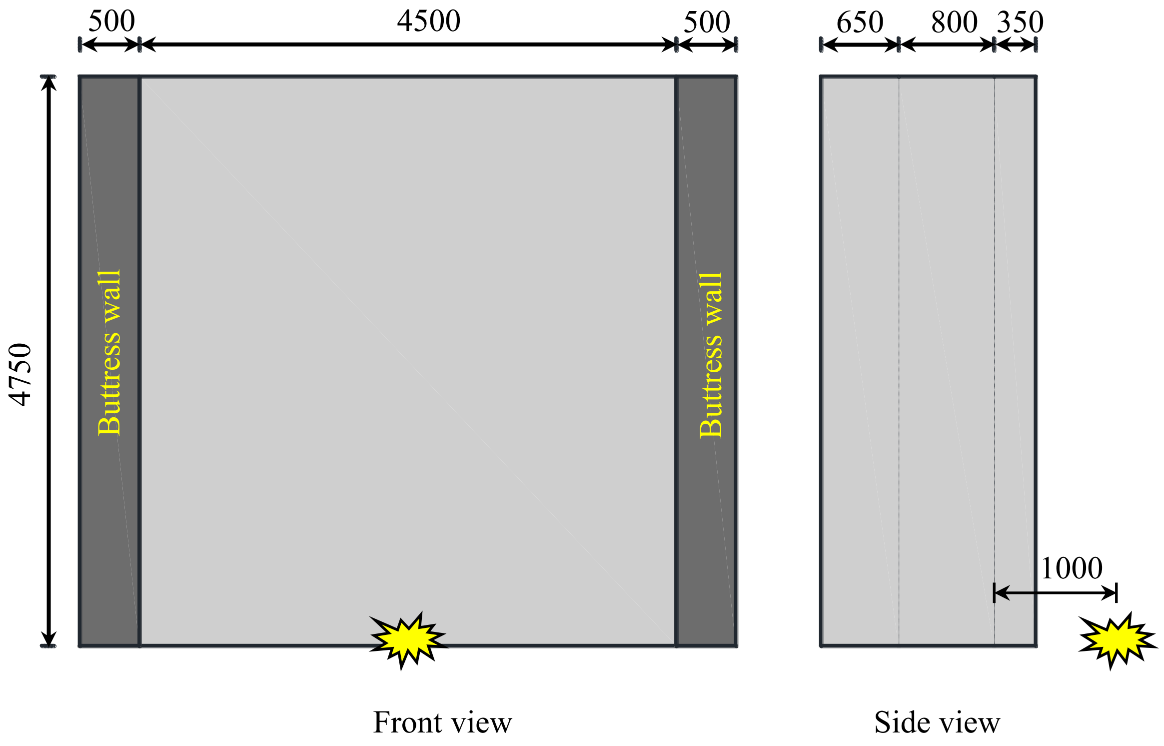


Threat parameter 1 (Minimum explosive at 1m from the wall)

# Prestressed Concrete (PSC) Wall with BFRP Strands

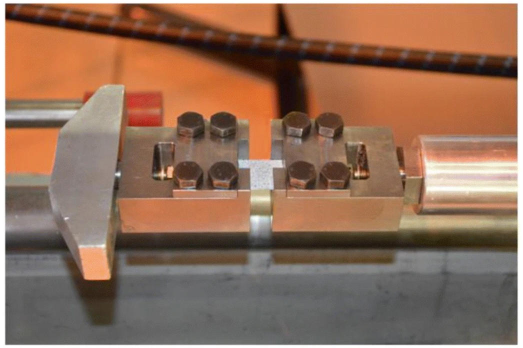

(a)

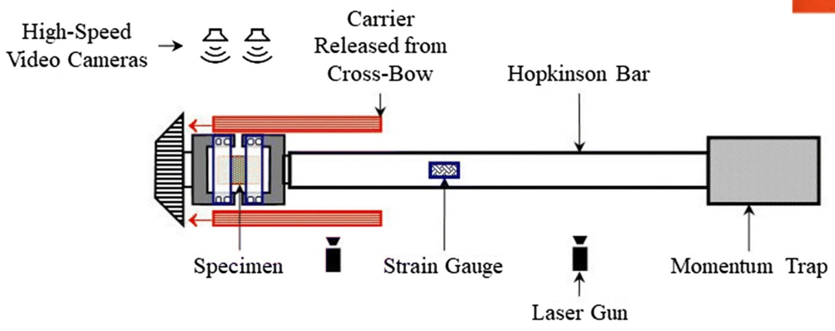


(b)

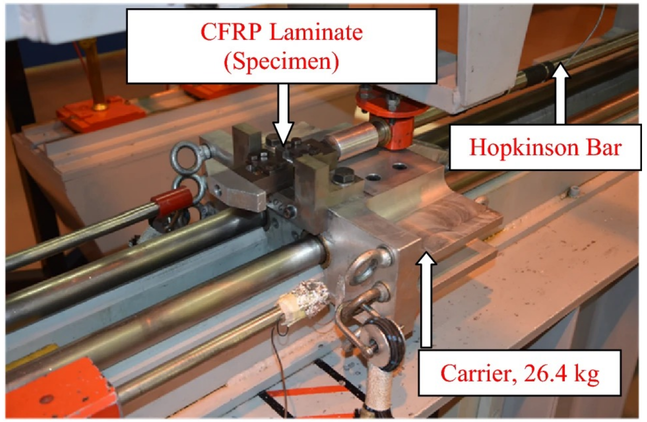


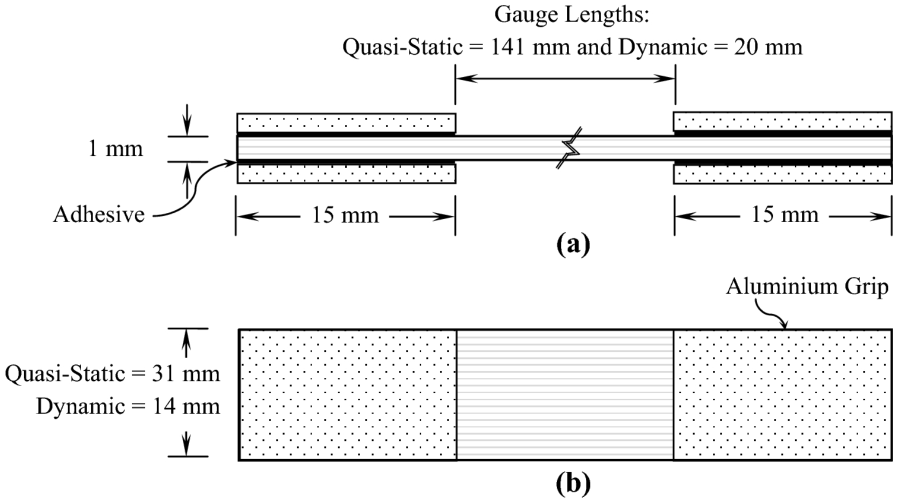


(a) Experimental setup of crossbow system with CFRP specimen in position, (b) typical sketch of the crossbow configuration employed for high strain rate tensile testing

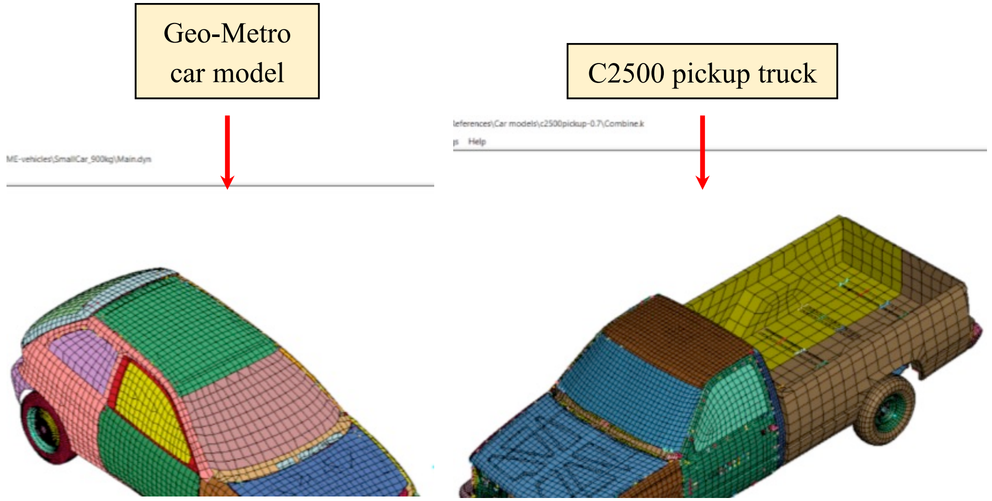


Threat parameter: (PSC wall subjected to vehicle with explosive)

# Prestressed Concrete (PSC) Wall with BFRP Strands

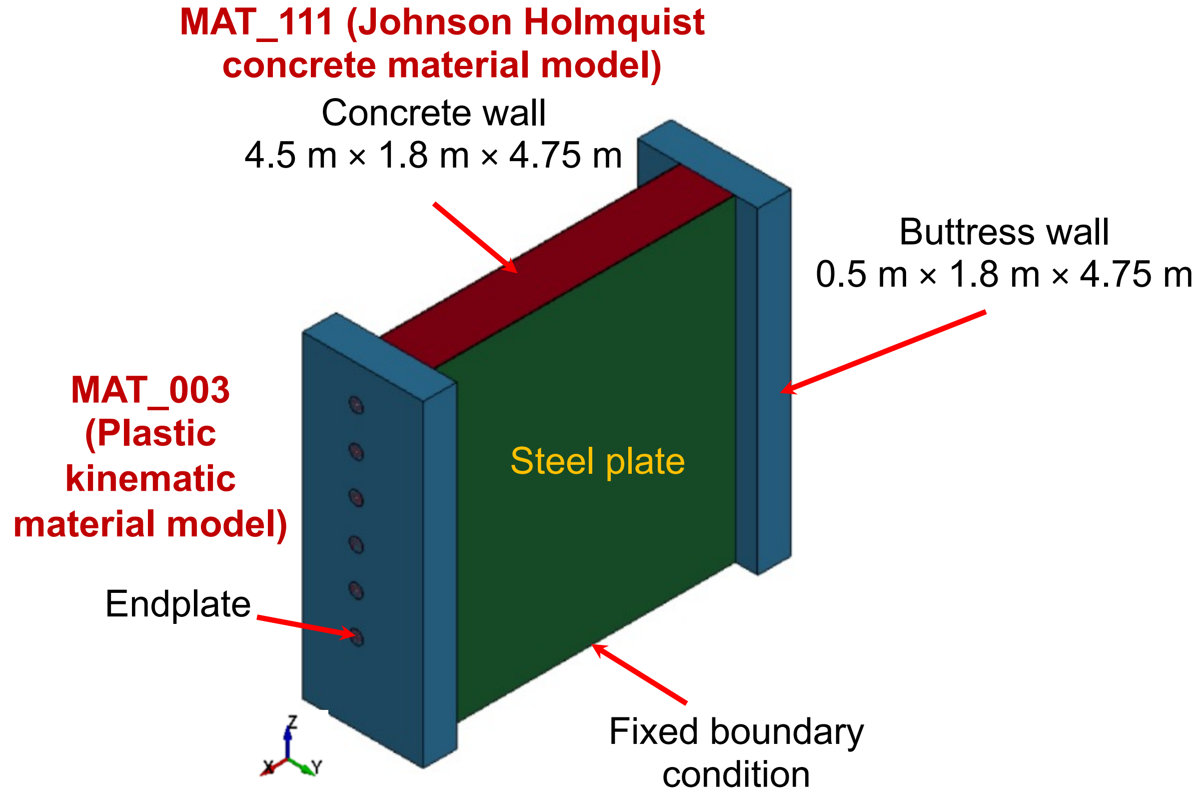


Isometric view of reinforced concrete wall FE model in LS-DYNA®

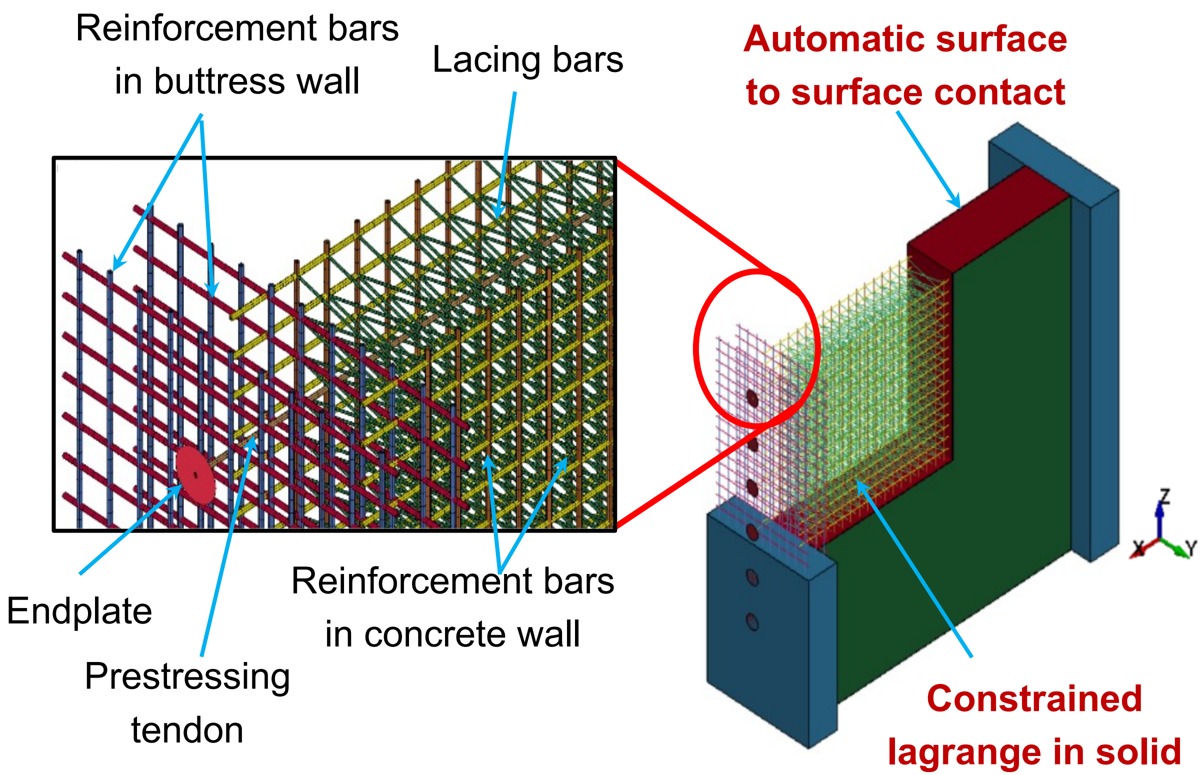


Reinforcement detailing in the reinforced concrete wall FE model in LS-DYNA®

# Prestressed Concrete (PSC) Wall with BFRP Strands

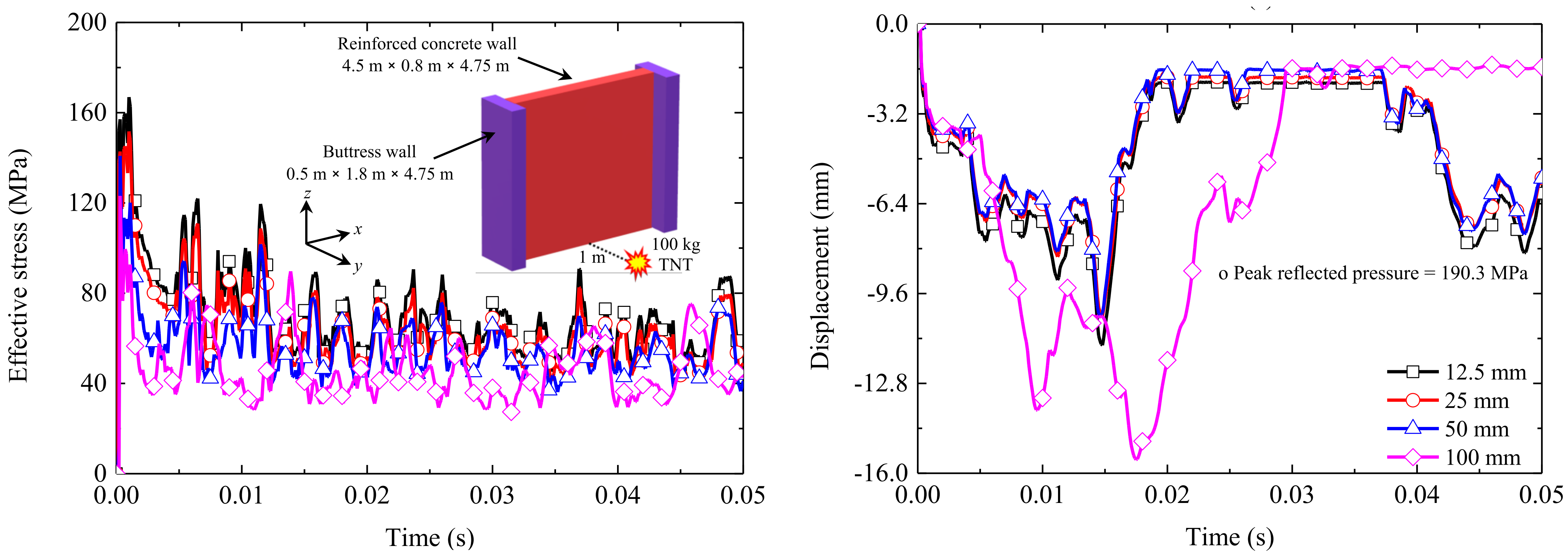


Mesh convergence study for a wall subjected to blast load with respect to effective stress and displacement time history

# Prestressed Concrete (PSC) Wall with BFRP Strands

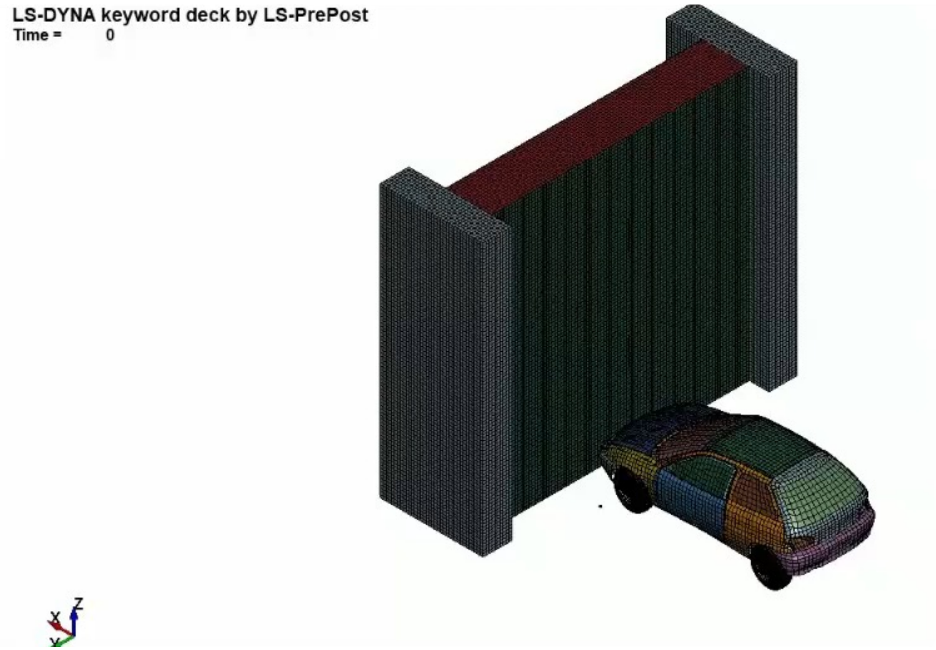


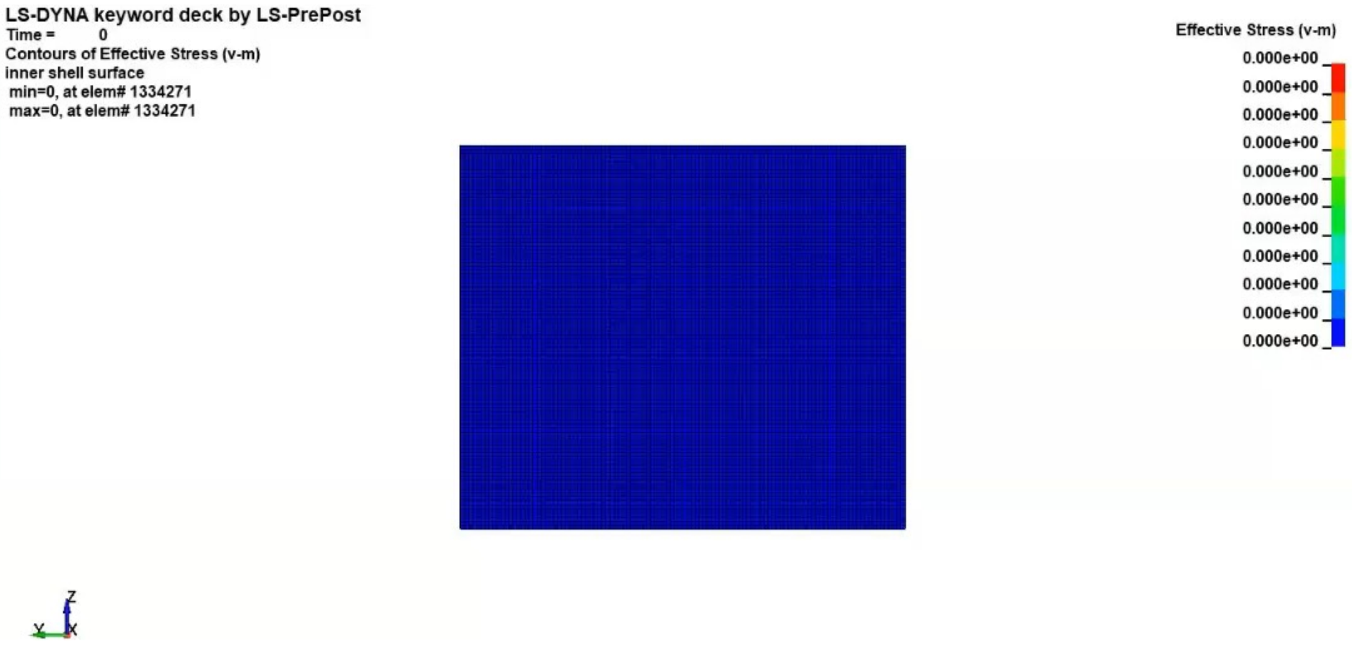


**PSC wall subjected to impact with car and the corresponding effective stress generated in the wall**

# Prestressed Concrete (PSC) Wall with BFRP Strands

## Validation with study reported by Neuberger et al. (2009) and Narayanmurthy et al. (2014)

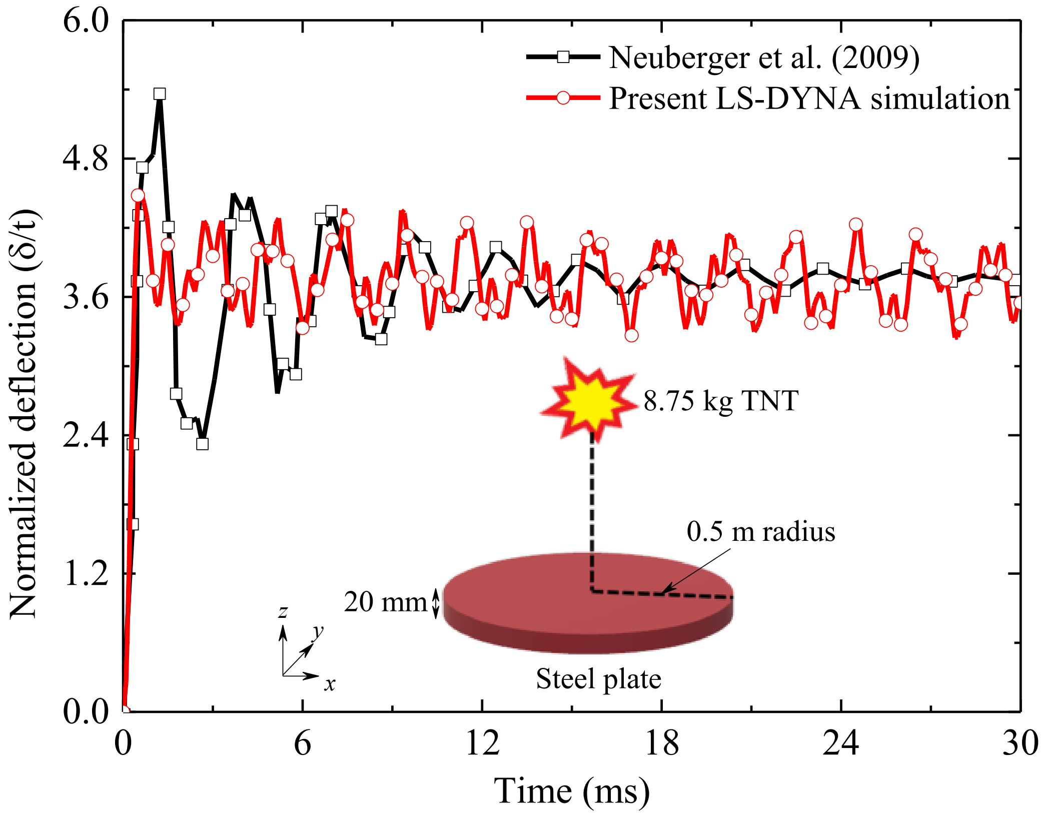


Comparison of normalized deflection time history between results reported by Neuberger et al. (2009) and present LS-DYNA® simulation

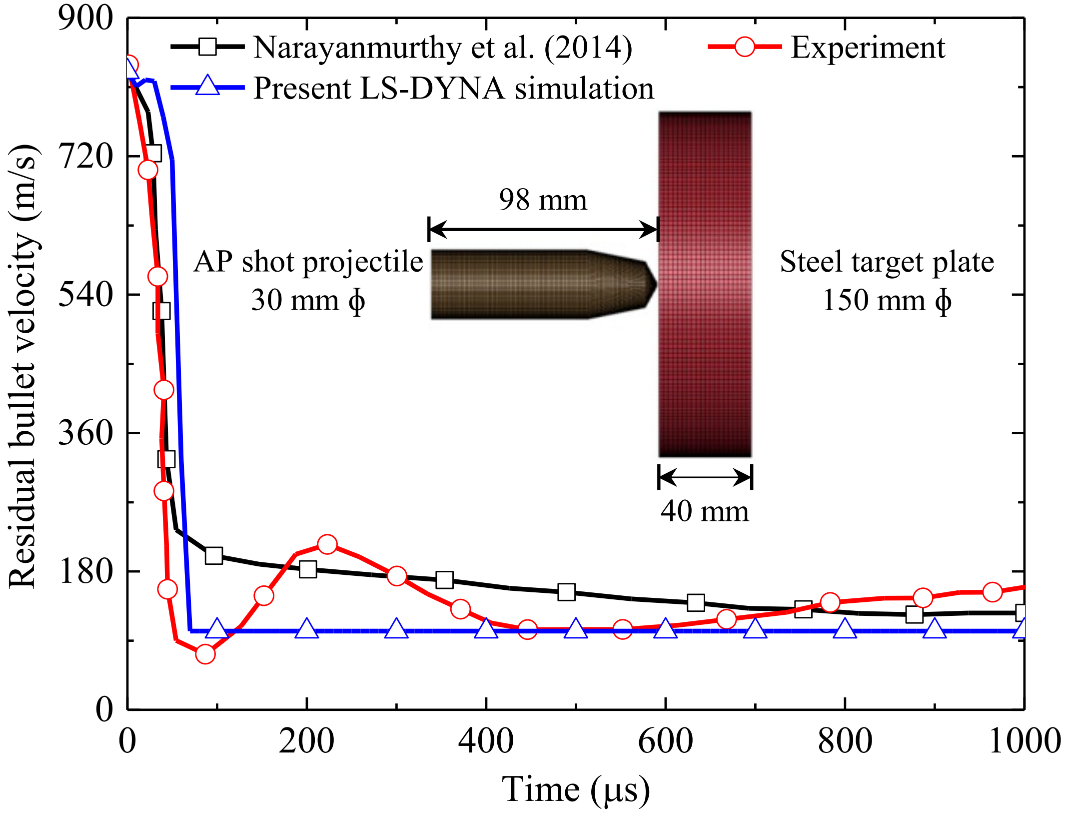


Comparison of residual bullet velocity between Narayanmurthy et al. (2014), experimental test result, and LS-DYNA® simulation

# Prestressed Concrete (PSC) Wall with BFRP Strands

| Reinforcement | Prestress | 100 kg | 200 kg | 300 kg | 400 kg | 500 kg |
|---|---|---|---|---|---|---|
| BFRP | ✗ | 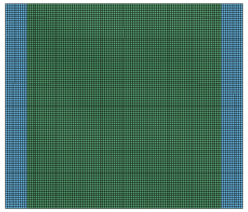 | 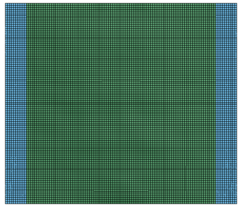 | 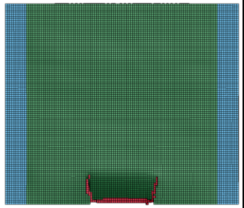 | 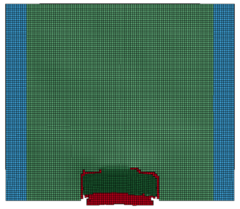 | 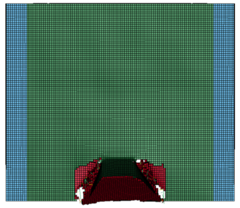 |
| BFRP | ✓ | 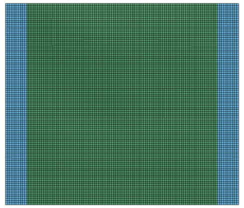 | 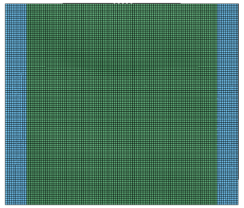 | 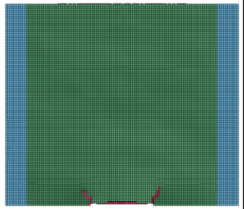 | 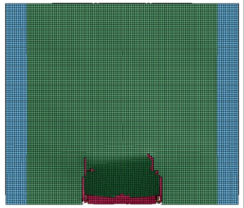 | 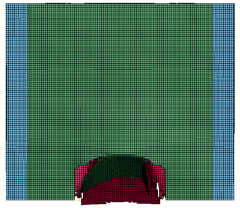 |
| Steel | ✗ | 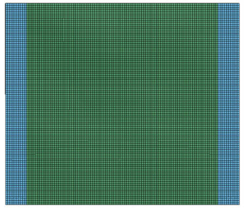 | 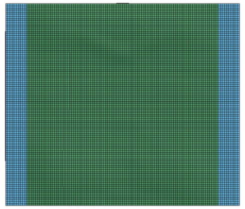 | 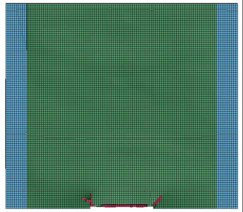 | 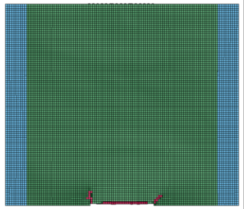 | 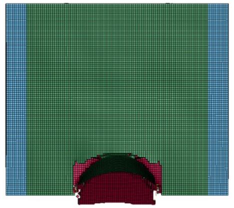 |
| Steel | ✓ | 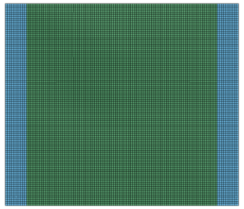 | 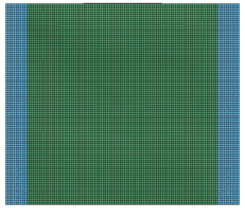 | 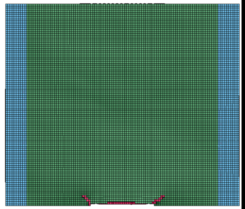 | 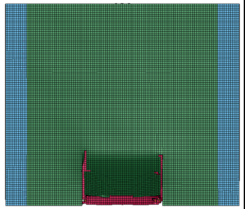 | 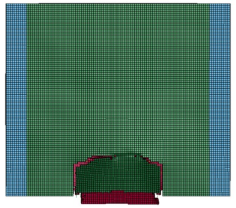 |

# Prestressed Concrete (PSC) Wall with BFRP Strands

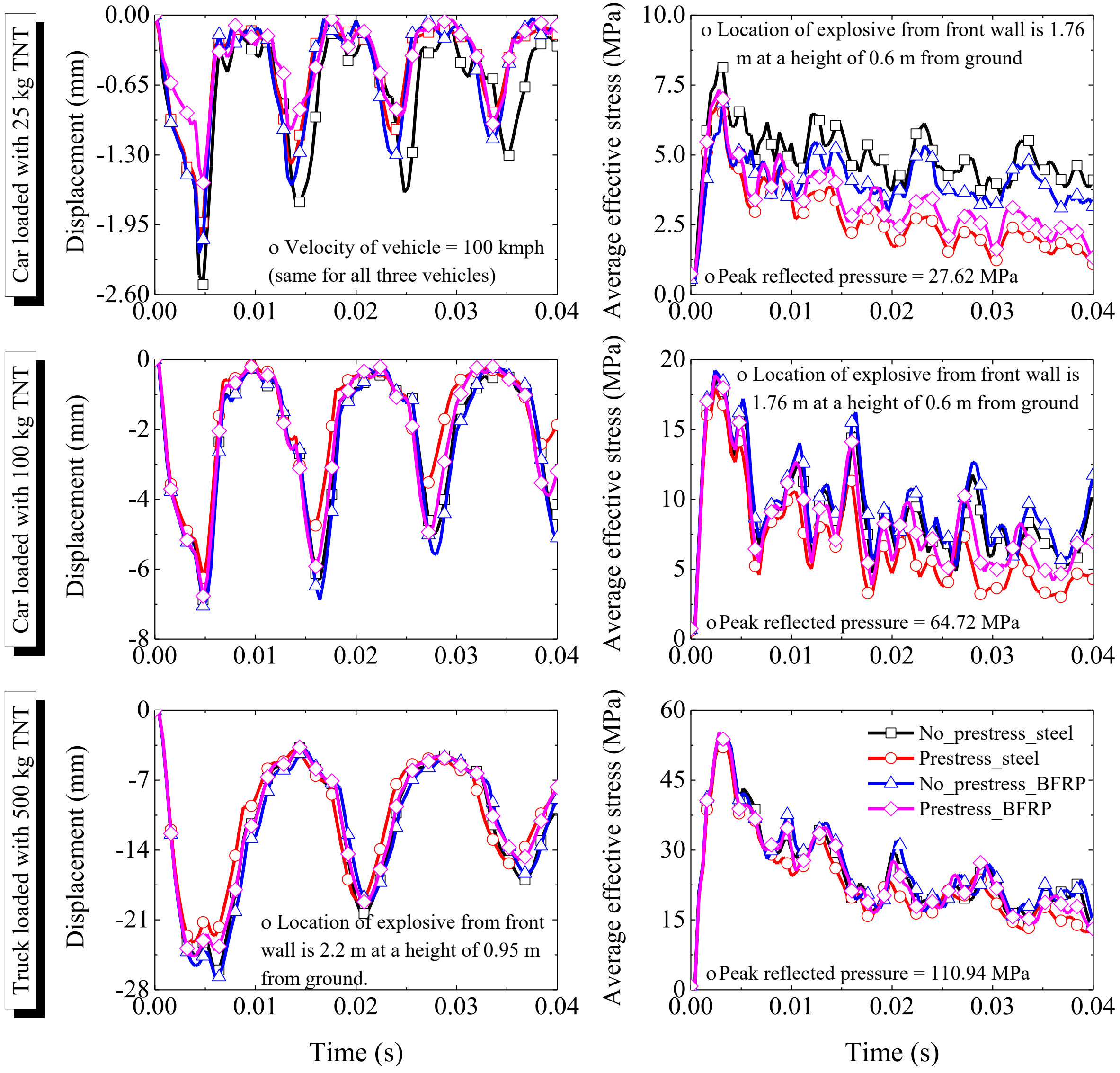


Response of PSC wall for three vehicles with explosive with prestressed and non-prestressed configurations having steel or BFRP reinforcement

# Prestressed Concrete (PSC) Wall with BFRP Strands

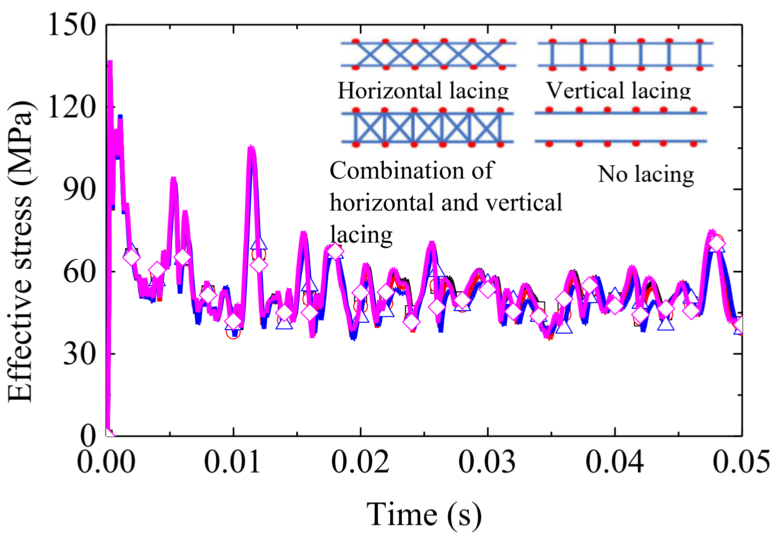


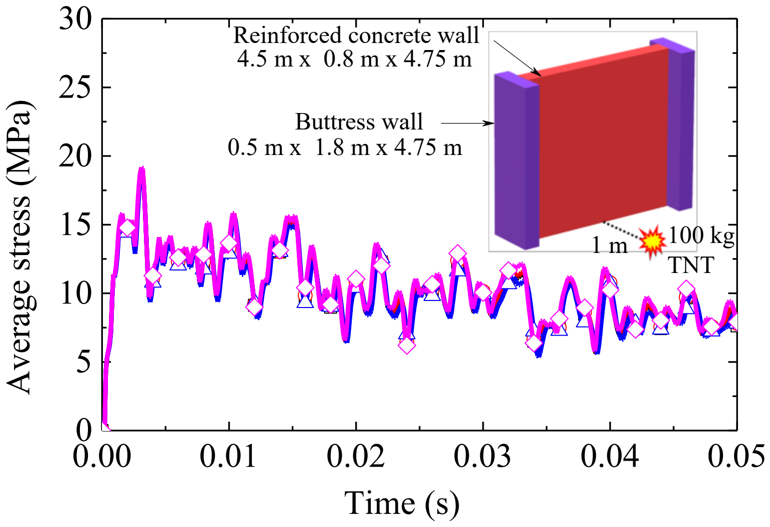


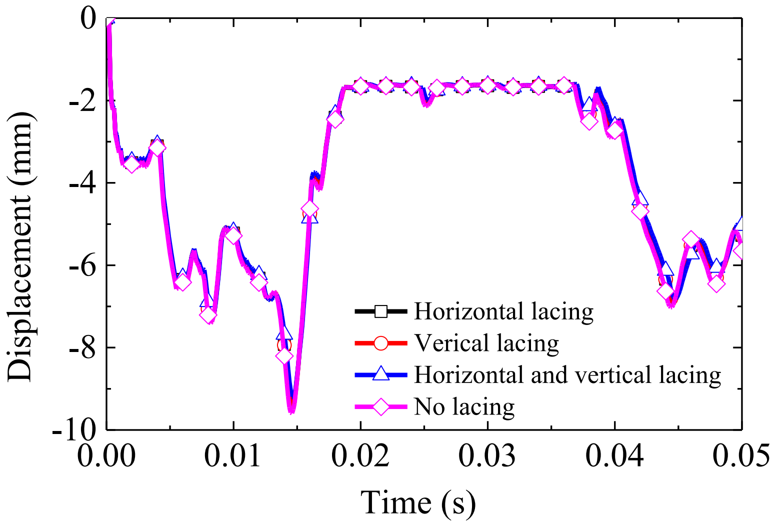


Study on different lacing configurations based on the effective stress, average stress, and displacement time history

Root mean square error between various lacing configurations

| Comparison parameter | Root mean square error | | |
|---|---|---|---|
| | Horizontal lacing | Vertical lacing | Combination of horizontal and vertical lacing |
| Displacement | 0.11 | 0.106 | 0.21 |
| Effective stress | 2.48 | 2.81 | 5.21 |
| Average effective stress | 0.503 | 0.445 | 0.89 |

# Prestressed Concrete (PSC) Wall with BFRP Strands

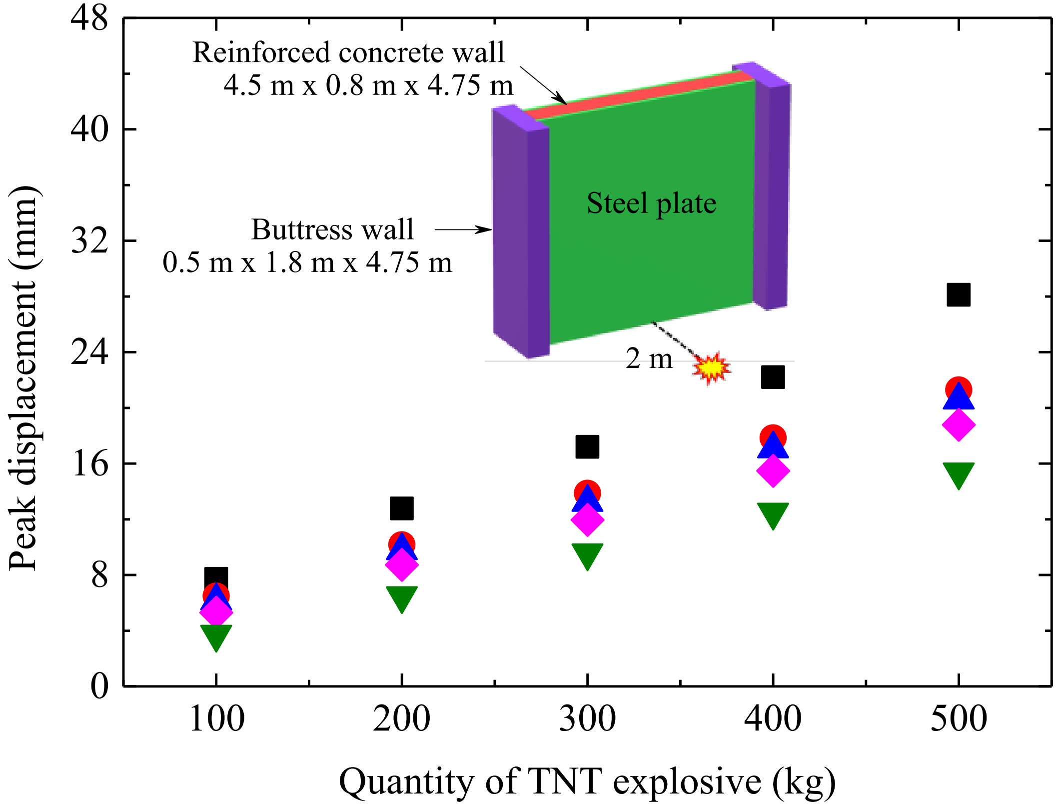


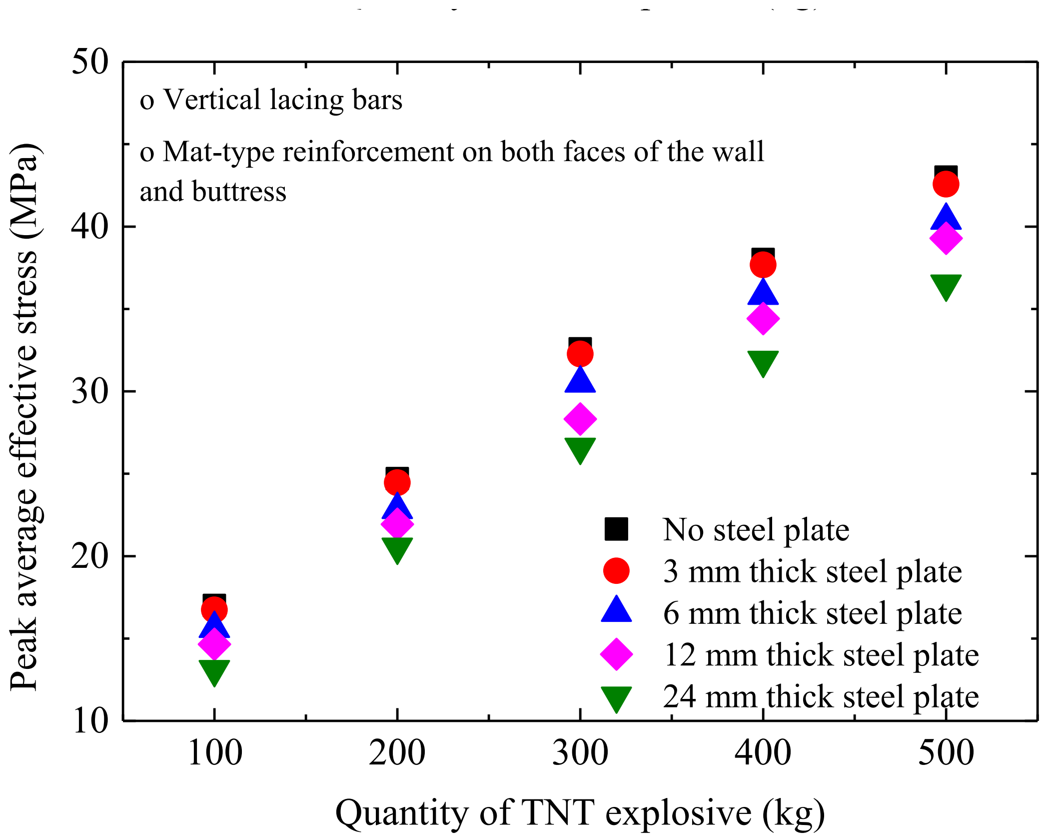


Effect of thickness of steel plate on blast performance of reinforced concrete wall based on peak displacement values and peak average effective stress

# Modular Structure with CFRP and XPS

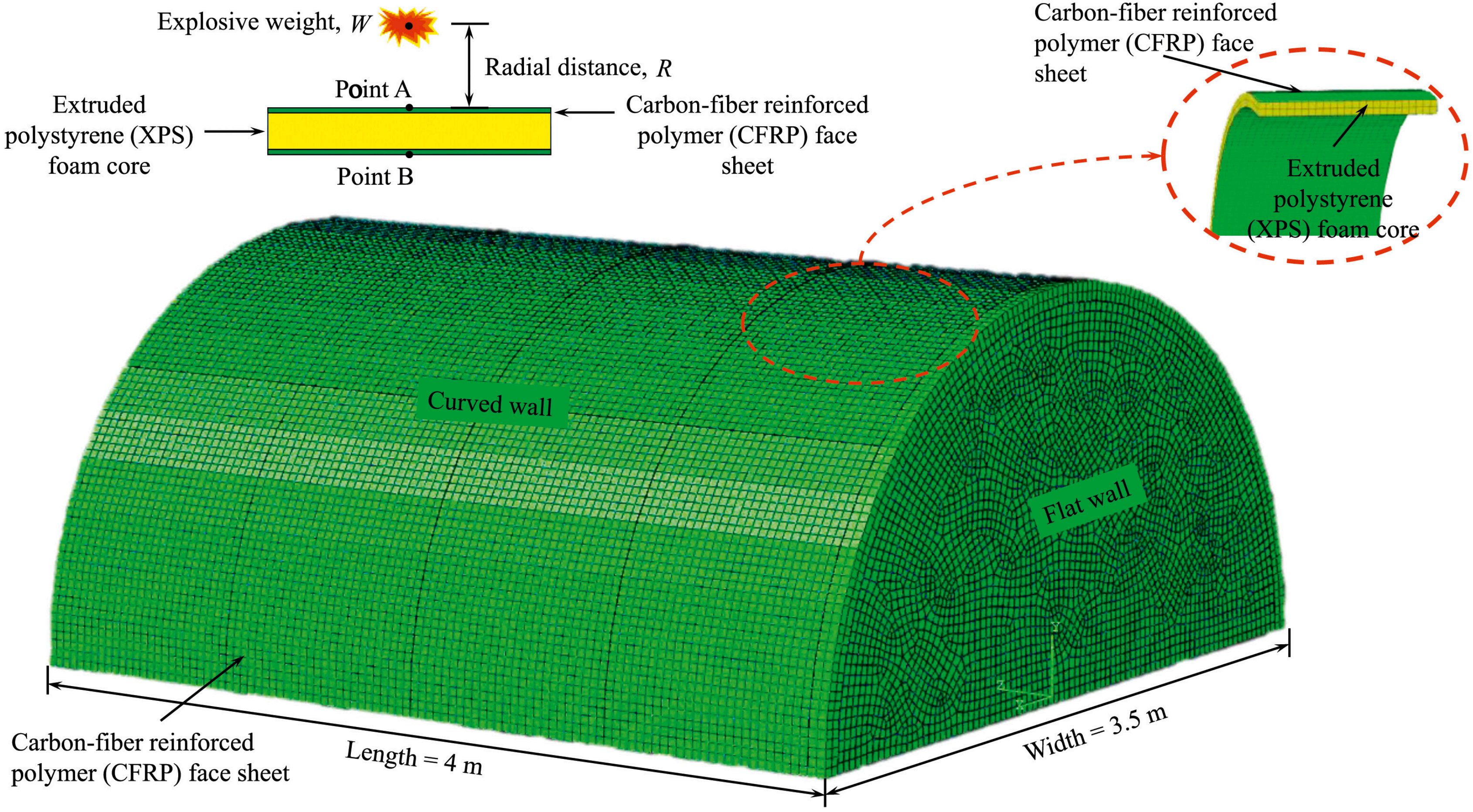


Modular CFRP and XPS sandwich composite structure

The three-dimensional (3D) finite element (FE) model of carbon fiber-reinforced polymer (CFRP) and extruded polystyrene (XPS) foam sandwich modular structure

# Conclusions and Future Directions

- Engineered (lightweight) composite materials, i.e., fiber reinforced laminated composite plates, FRP composite sandwich panels, etc. are efficient in blast resistant design.
- Concrete walls with fiber reinforced composite or FRP strengthening are better resilient against blast loads.
- Basalt fibers reinforced polymer (BFRP) composite can be used for resilient infrastructure design, specifically industrial structures where close-in detonation or contact blast scenario exists.
- Fiber reinforced composites can be efficiently used for retrofitting concrete slabs/ panels/ walls, beams, and columns more effectively with prestressing.
- <u>In future</u>: high strain rate characterization of the composite material constituents and field testing at close-in detonation condition and contact blast will be useful for numerical validation.

# Thank You

Discussion!
Questions?
Comments!

**Vasant Matsagar**
Professor, Dogra Chair, and Head
Department of Civil Engineering, Indian Institute of Technology (IIT) Delhi
Hauz Khas, New Delhi - 110 016, India
Cellphone: +91-98681-81807; E-Mail: matsagar@civil.iitd.ac.in
Homepage: http://www.matsagar.org